TECHNICAL NOTE 62-21

ON THE CALCULATION OF UNSTEADY INCOMPRESSIBLE LAMINAR BOUNDARY LAYERS OVER ARBITRARY CYLINDERS

KWANG-TZU YANG

CONTRACT NUMBER Nonr - 1623 (11)

DEPARTMENT OF MECHANICAL ENGINEERING
UNIVERSITY OF NOTRE DAME
NOTRE DAME, INDIANA

NOVEMBER, 1962

Technical Note 62-21

ON THE CALCULATION OF UNSTEADY INCOMPRESSIBLE LAMINAR BOUNDARY LAYERS OVER ARBITRARY CYLINDERS

by

KWANG-TZU YANG

CONTRACT NUMBER NONR-1623(11)

This research was carried out under the Bureau of Ships Fundamental Hydromechanics Research Program, S-R009 01 01, administered by the David Taylor Model Basin. Reproduction in whole or in part is permitted for any purpose of the United States Government.

Department of Mechanical Engineering
University of Notre Dame
Notre Dame, Indiana

November, 1962

TABLE OF CONTENTS

ABSTRACT

This report deals with the calculation of unsteady laminar boundary layers over arbitrary cylinders in an incompressible flow. The calculation procedure is based on an improved integral solution to the governing unsteady boundary-layer equations. The essential feature of this improved solution is to treat the usual integral solution as a first approximation, which is then used to linearize the governing equation in such a way that improved unsteady velocity profiles in the boundary layer are readily obtained. The integral solution is first described in detail, based on two assumed types of profiles, one being the well-known Pohlhausen's fourth-degree polynomial, and the other, an exponential function containing one arbitrary parameter. The basis of the improvement technique is then presented. Also introduced is a simple and convenient error criterion which is capable of indicating, without the knowledge of an exact solution, whether the improved solution is actually more accurate than the basic integral solution. Six numerical examples are then described to demonstrate the application of the improved integral solution and also to illustrate the use of the error criterion. Finally, it is concluded on the basis of the numerical results that in a general unsteady problem accurate results can be obtained by using the improved integral solution based on velocity polynomials within its whole range of validity, and that, outside of this range, the integral solution, based on exponential function, should be used with or without the im-

provement, depending on the relative magnitudes of the respective error quantities.

NOMENCLATURE

A	$(4/\xi^*)(\partial\bar{u}_\infty/\partial x^*)$
B	$(1/\xi^{*2})(\partial\xi^*/\partial t^*)$
C	$(\bar{u}_\infty/\xi^{*2})(\partial\xi^*/\partial x^*)$
c_f	local skin-friction coefficient, $\tau_w/(1/2\rho u_o^2)$
F	arbitrary function introduced in Equation (21)
F_1, F_2, F_3	universal functions defined in Equations (8)
f	dimensionless stream function in Equation (39)
G	form parameter in the exponential profile
g	function of t^*
H	ratio of displacement to momentum thicknesses
J	error criterion
K	universal function defined in Equations (8)
L	characteristic length of cylinder
P	$x^*/(\bar{u}_\infty t^*)$
P_1	function defined in Equation (29)
P_2	function defined in Equation (30)
R	Reynolds number, $u_o L/\nu$
t	time variable

t^*	$u_o t/L$
u,v	velocity components in the x- and y- directions, respectively
u^*	u/u_∞
u_o	reference velocity
$\bar{u}_\infty$	u_∞/u_o
x	distance coordinate along cylinder surface measured from forward stagnation point or from leading edge
x^*	x/L
y	distance coordinate normal to cylinder surface measured from surface
y^*	y/L
Z	$\delta_2{}^2/\nu$
Z^*	Zu_o/L
α	unsteadiness parameter
β	$\left[(2H/F_2)^{1/2}(\delta_2/\delta)\right]_{k=o}$
δ	a boundary-layer thickness
δ_2	momentum thickness
ϵ	error quantity defined in Equation (35)

η	y/δ
η_1	$y(u_\infty/\nu x)^{1/2}$
η_2	$y/2\sqrt{\nu t}$
λ	form parameter in the polynomial profile
μ	dynamic viscosity
ν	kinematic viscosity
ξ	function defined in Equations (7)
ξ^*	$\xi L/u_o$
ρ	density
τ_w	wall shear stress
ϕ	function of x^*

Subscripts:

i,j	grid points in Fig. 1
o	initial condition
o	basic integral solution
w	surface condition
∞	free-stream condition
I	region $0 \leq \eta \leq 1$
II	region $1 \leq \eta \leq \infty$

Superscript:

$'$ Derivatives with respect to the independent variable

INTRODUCTION

The two dimensional incompressible laminar boundary-layer theory for steady flows around cylinders is now well established in the literature. It is unfortunate, however, that the corresponding theory for unsteady flows is much less advanced, even though it is generally known that unsteady flow is physically more natural than flow under steady conditions, and that considerable physical insight to steady-flow behavior may be gained by studying unsteady boundary layers concerning coupled effects of vorticity diffusion away from the cylinder and fluid convection along the cylinder surface. The main difficulty is evidently the inclusion of the time variable in the governing laminar boundary-layer equations. Nevertheless, many significant investigations on unsteady laminar boundary layers have appeared in the literature, especially in recent years. A concise survey on this subject has recently been given by Stewartson [1].[1] Briefly, most published studies on unsteady laminar boundary layers may be grouped into six major areas. The well-known classical Rayleigh problem has now been extended to other infinite plate problems with more general boundary conditions [2-5].[2] Another area of study centers

---

[1] Numbers in brackets refer to References at the end of this report.

[2] No attempt is here made to quote all References.

on the prediction of the instant of onset of laminar separation for unsteady flow starting from rest, as undertaken by early workers in this field [6]. A third area of investigation concerns with exact solutions and possible exact solutions to the governing differential equations for a number of specific unsteady cases [7-11]. Furthermore, the leading-edge problem of unsteady flow over a semi-infinite plate has received much attention [12-14]. Also, very recently the effect of free-stream oscillation on laminar boundary-layer behavior has been studied in great detail by many investigators [15-22]. The last area of investigation deals with general unsteady laminar boundary layers over arbitrary cylinders [23-25].

In a recent study of hydrodynamic stability of unsteady laminar boundary layers over arbitrary cylinders, it has become apparent that, similar to the corresponding steady-flow problem, the stability characteristic would depend strongly on the second profile derivatives of the unsteady velocity profiles in the boundary layers, and consequently, accurate determination of these profile derivatives becomes necessary. For arbitrary cylinders and arbitrary free-stream unsteadiness, only approximate solutions are available in the literature. Both Schuh [24] and Yang [25] have developed one-parameter integral solutions to this general problem with the essential difference in the chosen profiles, with Schuh [24] utilizing a combination of Hartree's profiles for steady wedge flows and Pohlhausen's fourth-degree poly-

nomials, and Yang [25], profiles derived from exact similarity solutions for unsteady stagnation flows [9]. Even though these integral solutions do yield satisfactory overall unsteady laminar boundary-layer behaviors, there is considerable doubt that these approximate solutions would generally give second profile derivatives accurate enough for stability calculations, as this is a well known fact in the steady-flow theory.

This weakness of the integral solution, at least for steady compressible or incompressible flows, can be corrected to a very significant extent by an improvement technique developed recently [26,27]. Since the underlying idea of this technique applies equally well to the general unsteady laminar boundary-layer problem, there is good indication that it may be directly extended to the present problem to obtain improved unsteady velocity profiles. However, in view of the complexity introduced by the added time variable, such expectation can only be ascertained by detailed analysis of the unsteady problem and comparison of calculated results with known accurate solutions in the literature. The primary purpose of this report is to present such an analysis and the corresponding results, and in addition, it will also be shown that the general validity of this improved integral solution may be readily determined by an error criterion [27].

FORMULATION AND INTEGRAL SOLUTION

When an arbitrary two-dimensional cylinder moves unsteadily in an incompressible stagnant fluid, unsteady laminar boundary layer develops on the cylinder surface. In the incompressible-flow theory, this problem is exactly equivalent to one of the same fluid flowing over the stationary cylinder with the same unsteady velocity. Thus, with the coordinate system fixed on the cylinder, the well-known laminar boundary-layer equations may be written as follows:

$$\frac{\partial u}{\partial t} + u\frac{\partial u}{\partial x} + v\frac{\partial u}{\partial y} = \frac{\partial u_\infty}{\partial t} + u_\infty\frac{\partial u_\infty}{\partial x} + \nu\frac{\partial^2 u}{\partial y^2} \tag{1}$$

$$\frac{\partial u}{\partial x} + \frac{\partial v}{\partial y} = 0 \tag{2}$$

where x is the coordinate along the cylinder surface measured from the forward stagnation point or the leading edge, y the coordinate normal to the cylinder measured from the surface, u and v, velocity components in the x- and y-directions, respectively, t the time variable, ν the kinematic viscosity, and the subscript ∞ indicates conditions in the free stream. The initial condition generally depends on the specific problem, while the boundary conditions may be written as

$$\left.\begin{aligned} y = 0 \qquad & u = v = 0 \\ y \longrightarrow \infty \qquad & u \longrightarrow u_\infty(x,t) \end{aligned}\right\} \tag{3}$$

For arbitrary, but prescribed variations of $u_\infty(x,t)$, integral solutions based on somewhat different assumed velocity profiles have been presented by Schuh [24] and Yang [25]. The present analysis follows essentially the latter, except for some details, as will be shown later in the report. When the momentum equation (1), after eliminating v according to (2), is integrated across the boundary layer, the following well-known integral equation results:

$$\frac{\delta_2^2}{\nu}\frac{H}{u_\infty}\frac{\partial u_\infty}{\partial t} + \frac{\delta_2}{\nu}\frac{\partial(H\delta_2)}{\partial t} + u_\infty\frac{\delta_2}{\nu}\frac{\partial\delta_2}{\partial x}$$

$$+ (2 + H)\frac{\delta_2^2}{\nu}\frac{\partial u_\infty}{\partial x} = \frac{\tau_w\delta_2}{\mu u_\infty} \qquad (4)$$

where δ_2 is the usual momentum thickness, H the ratio of displacement to momentum thicknesses, τ_w the wall shear stress, and μ the viscosity. Now if we assume that the unsteady velocity can be represented by a one-parameter family of curves, i.e.

$$u^* = \frac{u}{u_\infty} = u^*(\lambda,\eta) \qquad (5)$$

where $\eta = y/\delta$, $\lambda = \lambda(\delta,u_\infty)$, and δ is an unsteady boundary-layer thickness, Equation (4) becomes a first-order partial differential equation for the unknown $\delta(x,t)$. In order to facilitate the solution to this equation, it may be conveniently cast in a simpler dimensionless form as follows [25]:

$$\bar{u}_\infty \frac{\partial K}{\partial x^*} + F_1 \frac{\partial K}{\partial t^*} = \xi^* \left[F_3 + K(C - A + HB) \right] \tag{6}$$

where

$$\left.\begin{aligned} K &= Z\xi \qquad Z = \frac{\delta_2^2}{\nu} \qquad \xi = \frac{\partial u_\infty}{\partial x} + \frac{1}{u_\infty}\frac{\partial u_\infty}{\partial t} \\ x^* &= \frac{x}{L} \qquad t^* = \frac{u_o t}{L} \qquad \xi^* = \frac{\xi L}{u_o} \qquad \bar{u}_\infty = \frac{u_\infty}{u_o} \\ A &= \frac{4}{\xi^*}\frac{\partial \bar{u}_\infty}{\partial x^*} \qquad B = \frac{1}{\xi^{*2}}\frac{\partial \xi^*}{\partial t^*} \qquad C = \frac{\bar{u}_\infty}{\xi^{*2}}\frac{\partial \xi^*}{\partial x^*} \end{aligned}\right\} \tag{7}$$

and u_o is a reference velocity, and L, a characteristic length of the cylinder. Furthermore, universal functions K, F_1, F_2 and F_3 are pure functions of the form parameter λ, which may be written as

$$\left.\begin{aligned} K &= \left(\frac{\delta_2}{\delta}\right)^2 \lambda \qquad F_1 = H + 2K\frac{dH}{d\lambda}\frac{d\lambda}{dK} \\ F_2 &= \frac{\tau_w \delta}{\mu u_\infty}\left(\frac{\delta_2}{\delta}\right) \qquad F_3 = 2F_2 - 2KH \end{aligned}\right\} \tag{8}$$

and in addition, H and (δ_2/δ) are also universal functions of the same parameter λ, provided that λ is specifically defined as

$$\lambda = \frac{\delta^2}{\nu}\xi \tag{9}$$

which obviously reduces to the Pohlhausen's form parameter for steady flows. It now becomes clear that even though K is explicitly written as the unknown in Equation (6), the form parameter λ is actually the unknown to be sought, in

view of the unique relation (8) between K and λ, once the velocity profile (5) is assumed.

Before solutions to Equation (6) can be attempted, it is necessary first to introduce specific profiles in the form of Equation (5) and to determine the corresponding universal functions. As already pointed out previously, Schuh's analysis [24] utilizes both the Pohlhausen's fourth-degree velocity polynomial (for $K<0$) and Hartree's profiles for steady wedge flows (for $K>0$), and Yang [25] has based his choice on the exact profiles for unsteady stagnation "hyperbolic time-variation" flows [9]. The obvious weakness in Schuh's choice is that the resulting universal functions are discontinuous at $K = 0$, and this point of discontinuity is expected to occur quite frequently in any general unsteady-flow problem. In addition, the Hartree's wedge-flow profiles, as well as the corresponding universal functions, are only known in tabulated forms, and hence cannot be manipulated readily. Yang's profiles, though continuous throughout the entire region of K, evidently suffer the same difficulty. However, since the present improved integral solution, as will be described in the next section, utilizes the integral solution as a first approximation, the velocity profiles and the associated universal functions from the integral solution must be manipulated. Consequently, all these available unsteady profiles are not suitable for the present use. In the present study, two distinctly different profiles have been considered. One is still the Pohlhausen's fourth-degree

polynomial, which, however, is allowed to be valid in the range $-12 \leq \lambda \leq +12$, with the lower limit corresponding to laminar separation. For $\lambda > 12$, the velocity polynomial becomes non-sensible, and hence is to be replaced by an exponential profile. This discontinuity is not expected to be too serious in actual applications, since it only occurs in a region of large values of ξ, corresponding to very large acceleration in the free stream. Now the details of these two assumed profiles are separately described.

The Pohlhausen's fourth degree polynomial for the velocity profile is well known, and may be written as

$$\left.\begin{aligned} u^* &= \eta(2 - 2\eta^2 + \eta^3) + \frac{\lambda}{6}\eta(1-\eta)^3 \qquad 0 \leq \eta \leq 1 \\ u^* &= 1 \qquad\qquad\qquad\qquad \eta \geq 1 \end{aligned}\right\} \tag{10}$$

from which universal functions in (8) can be readily determined, resulting in

$$\left.\begin{aligned} K &= \left(\frac{37}{315} - \frac{\lambda}{945} - \frac{\lambda^2}{9072}\right)^2 \lambda \qquad \frac{\delta_2}{\delta} = \frac{37}{315} - \frac{\lambda}{945} - \frac{\lambda^2}{9072} \\ H &= \frac{\frac{3}{10} - \frac{\lambda}{120}}{\frac{37}{315} - \frac{\lambda}{945} - \frac{\lambda^2}{9072}} \qquad F_2 = \left(2 + \frac{\lambda}{6}\right)\left(\frac{37}{315} - \frac{\lambda}{945} - \frac{\lambda^2}{9072}\right) \\ F_1 &= H + \frac{-\frac{\lambda}{60}\left(\frac{37}{315} - \frac{\lambda}{945} - \frac{\lambda^2}{9072}\right) + \frac{\lambda}{1575} + \frac{13\lambda^2}{113400} - \frac{\lambda^3}{272160}}{\left(\frac{37}{315} - \frac{\lambda}{945} - \frac{\lambda^2}{9072}\right)\left(\frac{37}{315} - \frac{\lambda}{315} - \frac{5\lambda^2}{9072}\right)} \\ F_3 &= 2\left(\frac{37}{315} - \frac{\lambda}{945} - \frac{\lambda^2}{9072}\right)\left(2 - \frac{2}{15}\lambda + \frac{\lambda^2}{120}\right) \end{aligned}\right\} \tag{11}$$

Outside the region of validity of the above polynomial, Equation (10) is to be replaced by an exponential function, which has been utilized in both steady- and unsteady-flow cases [28,29,3] with high degree of success especially in the unsteady-flow problems. It is in the following form:

$$u^* = 1 - e^{-\eta}(1 - G\eta) \qquad 0 \leqslant \eta \leqslant \infty \tag{12}$$

where $\eta = y/\delta$ and the form parameter G plays the same role as λ in the Pohlhausen's polynomial. It should be emphasized here that the boundary-layer thickness δ in Equation (12) has no relation whatever to that in Equation (10). In addition, physically sensible profiles are only obtainable for negative G values, with $G = -1$ for laminar separation. It is also seen that boundary conditions at infinity are automatically satisfied, and the relationship between G and δ can be easily obtained from evaluating the momentum equation (1) at the wall, i.e.

$$1 + 2G = \frac{\delta^2}{\nu}\xi \tag{13}$$

Now once the profile is known, the corresponding universal functions may again be determined explicitly. They are shown as follows:

$$\left.\begin{aligned} K &= (1 + 2G)\left(\frac{1}{2} - \frac{G}{2} - \frac{G^2}{2}\right)^2 \qquad \frac{\delta_2}{\delta} = \frac{1}{2} - \frac{G}{2} - \frac{G^2}{4} \\ H &= \frac{4(1 - G)}{2 - 2G - G^2} \qquad F_2 = \frac{1}{4}(1 + G)(2 - 2G - G^2) \\ F_1 &= \frac{12}{8 + 5G} \qquad F_3 = G^2(2 - 2G - G^2) \end{aligned}\right\} \tag{14}$$

Now solution to the unsteady integral equation is considered. Equation (6) is a linear first-order partial differential equation, the most general solution of which is by the method of characteristics. However, this method yields exact solutions to Equation (6) only in those cases where two integrable equations can be obtained from the corresponding characteristic equations. For general unsteady free-stream velocity distribution, other means of solution must be used instead. In view of the above, problems of special interest may be grouped into the following classes, relative to different geometry and methods of solution:

1. Stagnation Flow with Free-Stream Velocity Varying Arbitrarily with Time

For this class of problems, the free-stream velocity distribution may be written as

$$\bar{u}_\infty = \left[x^* g(t^*)\right]_{x^* \longrightarrow 0}$$

where g is an arbitrary, but continuously differentiable function of time. With ξ^*, A and B given by pure functions of t^* and $C = 0$, Equation (6) reduces to

$$\frac{dK}{dt^*} = \frac{\xi^*}{F_1}\left[F_3 + K(HB-A)\right] \tag{15}$$

which may be conveniently solved numerically for the unknown λ or G, depending on the profiles chosen, in terms of certain initial condition. For instance, if $g(0) = 1$, corresponding to initially steady motion, then $\lambda(0)$ and $G(0)$ can be determined from steady-flow theory.

2. Flow over an Infinite Plate with Free-Stream Velocity Varying Arbitrarily with Time

With $\bar{u}_\infty = g(t^*)$ and all derivatives with respect to x^* neglected, it may be readily shown that Equation (6) now assumes the following form:

$$\frac{dK}{dt^*} = \frac{\xi^*}{F_1}\left[F_3 + BHK\right] \tag{16}$$

where both ξ^* and B are now pure functions of t^*. The above equation may again be numerically integrated in terms of any specific initial condition depending on the physical problem under consideration, resulting in either $\lambda(t^*)$ or $G(t^*)$. It may be pertinent to mention here that the corresponding problem of unsteady flow over a semi-infinite plate presents some difficulty regarding its solution. It must be solved in the same manner as a general problem of an arbitrary cylinder in an arbitrarily unsteady flow, as will be described later. One exception is the case of a semi-infinite plate moving from rest with a constant acceleration. The corresponding integral equation (6) has a similarity solution satisfying the following ordinary equation [24,25]

$$\frac{dK}{dP} = \frac{2F_2 - 3KH}{1 - 2PF_1} \tag{17}$$

where $P = x^*/(\bar{u}_\infty t^*)$, which is subjected to the boundary conditions $K(0) = 0$ and $K(\infty) = K_o$, where the constant K_o is determined from

$$3K_oH(K_o) = 2F_2(K_o) \tag{18}$$

Since only one boundary condition is necessary, solution to Equation (17) is obtained by matching the two solutions satisfying the two boundary conditions at a proper value of F. Other details of this problem will be shown in a later section. Another exception is for flow over a semi-infinite plate with step-change in free-stream velocity. Since for this problem K is identically zero, all universal functions become constants, and Equation (6) in this limit reduces to

$$\bar{u}_\infty \frac{\partial Z^*}{\partial x^*} + H \frac{\partial Z^*}{\partial t^*} = 2F_2 \tag{19}$$

where $Z^* = Zu_o/L$. This equation may be conveniently solved by the method of characteristics. The corresponding characteristic equations are then given by

$$\frac{dx^*}{\bar{u}_\infty} = \frac{dt^*}{H} = \frac{dZ^*}{2F_2} \tag{20}$$

from which two integrable equations may be readily obtained. After eliminating the two arbitrary constants of integration, we obtain the general solution

$$Z^* - \frac{2F_2}{H} t^* = F\left(x^* - \frac{\bar{u}_\infty}{H} t^*\right) \tag{21}$$

where the arbitrary function F is determined from the initial and boundary conditions. For a flow starting from rest, the conditions $Z^*(x^*,0) = 0$ and $Z^*(0,t^*) = 0$ must all be satisfied. Hence Equation (21) becomes

$$Z^* = \frac{2F_2}{H} t^* \qquad 0 \leq t \leq \frac{H}{\bar{u}_\infty} x^* \tag{22a}$$

$$Z^* = \frac{2F_2}{\bar{u}_\infty} x^* \qquad t^* \geqslant \frac{H}{\bar{u}_\infty} x^* \tag{22b}$$

where Equation (22a) indicates the transient behavior, while Equation (22b), the steady-state solution. When the flow changes from an originally steady-state condition, we have accordingly $Z^*(x^*,0) = Z_o^*(x^*)$ and $Z^*(0,t^*) = 0$. A similar analysis yields

$$\left.\begin{aligned} Z^* &= \frac{2F_2}{H}\left[\frac{H}{\bar{u}_{\infty i}} x^* + \left(1 - \frac{\bar{u}_\infty}{\bar{u}_{\infty i}}\right) t^*\right] \qquad 0 \leqslant t^* \leqslant \frac{H}{\bar{u}_\infty} x^* \\ Z^* &= \frac{2F_2}{\bar{u}_\infty} x^* \qquad\qquad t^* \geqslant \frac{H}{\bar{u}_\infty} x^* \end{aligned}\right\} \tag{23}$$

where $\bar{u}_{\infty i}$ is the initial steady free-stream velocity, which may be taken as unity without loss of generality.

3. Arbitrarily Unsteady Flow over Arbitrary Cylinders

The validity of the method of characteristics as applied to this general problem has been implicitly assumed by Schuh [24]. However, limitations to this method were not pointed out, nor was any example illustrating this application to a general unsteady problem given. Yang [25] later has proposed a step-by-step calculation procedure, also based on the method of characteristics, to this general problem. Unfortunately, a close examination of this procedure reveals that it yields accurate results only in cases where the quantity $\partial K/\partial x^*$ is a weak function of t^*. In the present study, a new calculation procedure is introduced, which has the capability of obtaining numerical solution to Equation (6) as accurately as desired. This procedure is based on a lumped approximation of the variation of K with respect to x^*. If we now con-

sider the grid system in the $x^* - t^*$ plane as shown in Fig. 1, it is seen that the derivative $\partial K/\partial x^*$ at any point may be conveniently approximated by

$$\left(\frac{\partial K}{\partial x^*}\right)_{t^* = j\Delta t^*} = \frac{K_{i+1,j} - K_{i-1,j}}{2\Delta x^*} \tag{24}$$

which involves an error of the order of $(\Delta x^*)^2$. The integral equation (6) may now be written as

$$\frac{\partial K}{\partial t^*} = \frac{\xi^*}{F_1}\left[F_3 + K(C - A + HB)\right] - \frac{\bar{u}_\infty}{F_1}\left(\frac{\partial K}{\partial x^*}\right) \tag{25}$$

For a given problem, some initial condition $K(x^*,0)$ must be known. For a flow starting from rest, $K(x^*,0) = K_0$, which must be determined from a limiting process similar to that of obtaining Equation (18) [25]. When the flow is initially steady, $K(x^*,0)$ may then be evaluated from the steady-flow theory. Before solution to Equation (25) is considered, it is first necessary to obtain $K(0,t^*)$. For a blunt-nosed cylinder, $K(0,t^*)$ is obtained by directly integrating Equation (25) with $\bar{u}_\infty = 0$, which is evidently identical to Equation (15). When the cylinder has a sharp leading edge, $K(0,t^*)$ becomes identically zero. Once $K(x^*,0)$ and $K(0,t^*)$ are known, solution to Equation (25) may then proceed as follows[3]: Since at $t^* = 0$ the derivative $\partial K/\partial x^*$ is known exactly, there is no need to evaluate this quantity from Equation (24). From the given unsteady free-stream

[3] In actual applications, it is desirable to treat either λ or G as the dependent variable, instead of K, in view of the fact that all universal functions are explicit functions of λ or G.

velocity distribution, quantities such as ξ^*, A, B, C and $\bar{u}_\infty$ may then be evaluated at this instant. Consequently, now the right-hand side of Equation (25) can be determined accordingly for all points along the x^*-axis (Fig. 1). Then one step of numerical integration with respect to t^* at each of these points immediately yields $K(x^*,\Delta t^*)$. In this regard, it has been found that the usual Runge-Kutta integration routine, which is accurate to the order of $(\Delta t^*)^4$, is very satisfactory. Together with the known value of $K(0,\Delta t^*)$, derivatives $(\partial K/\partial x^*)$ at $t^* = \Delta t^*$ may now be evaluated for all points along the x^*-axis according to (24). This process is then repeated for successive time instants until a desired time elapse is covered. It is noted that this step-by-step calculation procedure has one advantage over that of pure finite-difference numerical approximations in both x^* and t^*, and that is that here the question of stability of the numerical solution never arises. Furthermore, the present procedure can be conceivably improved in its accuracy by using a higher-order differentiation formula than that in Equation (24).

Once the parameter K becomes a known function of x^* and t^*, the corresponding form parameter λ or G can be evaluated, yielding $\delta = \delta(x^*,t^*)$. Equation (10) or (12) then immediately gives the unsteady velocity profiles. Thus, the integral solution may now be considered as complete.

AN IMPROVED INTEGRAL SOLUTION AND A RELATED ERROR CRITERION

As generally recognized in the application of Karman-Pohlhausen's integral procedure, there are two essential weaknesses which give rise to the inaccuracy of the approximate solution. One is that the governing partial differential equation is only satisfied in the mean, and the other, that the choice of assumed profiles is entirely arbitrary, and the resulting accuracies of different types of profiles could be different by significant amounts. In the laminar boundary-layer theory, most earlier improvements for general problems have been based either on the choice of novel profiles or on the use of additional integral equations, or sometimes known as moment equations. Unfortunately, none of these improvements has general validity to arbitrary problems. This has led the present writer to develop an essentially different improvement technique for the general laminar boundary-layer problem [26] in an attempt to correct significantly the aforementioned weaknesses of the basic integral solution. This technique basically utilizes the integral solution as a first approximation, which, when substituted into the governing differential equation, linearizes the equation, which may then be readily solved for the improved profiles in closed forms. In view of its apparent success, this technique has since been extended to other physical problems [30,31]. Very recently, it has been further improved in a minor detail in that now the boundary condition at infinity is exactly satisfied, and in addition a simple error criterion is introduced such that validity of the improvement can be readily

determined without knowledge of the exact solution [27]. As mentioned previously, this improvement technique has only so far been developed for a parabolic-type of partial differential equations in two independent variables. Its extension to equations with three independent variables raises some uncertainties. The primary purpose of this section is to present the detailed analysis of this extension to the general unsteady boundary-layer problem in two-dimensional incompressible flow. To simplify the presentation, the following will be described only for the integral solution based on Pohlhausen's velocity polynomial. However, the formulation of the improved procedure may be easily extended to cases where exponential profiles (12) are used. In fact, it is only necessary to replace the form parameter λ by the quantity $(1 + 2G)$ in view of Equation (13) and the usual definition of λ. Neverthless, significant differences will be pointed out, whenever desirable.

From the basic integral solution as described previously, both λ and δ become known functions of x^* and t^*. In order to facilitate the linearization of the governing differential equations by introducing the integral solution, it is now desirable to transform these equations from the (x,y,t) coordinate system to the (λ,η,t^*) system. This transformation is governed by

$$\left.\begin{aligned}
\frac{\partial}{\partial x} &= \frac{\partial \lambda}{\partial x}\frac{\partial}{\partial \lambda} + \frac{1}{\delta}\frac{\partial \delta}{\partial x}\eta\frac{\partial}{\partial \eta} \\
\frac{\partial}{\partial t} &= \frac{\partial \lambda}{\partial t}\frac{\partial}{\partial \lambda} - \frac{1}{\delta}\frac{\partial \delta}{\partial t}\eta\frac{\partial}{\partial \eta} + \frac{u_o}{L}\frac{\partial}{\partial t^*} \\
\frac{\partial}{\partial y} &= \frac{1}{\delta}\frac{\partial}{\partial \eta}
\end{aligned}\right\} \qquad (26)$$

The continuity equation (2) is first considered. Solving for v and transforming, we have

$$v = -\int_0^y \frac{\partial u}{\partial x} dy$$

$$= -\delta u_\infty \left[\left(\frac{1}{u_\infty}\frac{\partial u_\infty}{\partial x} + \frac{1}{\delta}\frac{\partial \delta}{\partial x}\right)\int_0^\eta u^* d\eta - \frac{1}{\delta}\frac{\partial \delta}{\partial x}\eta u^* + \frac{\partial \lambda}{\partial x}\frac{\partial}{\partial \lambda}\int_0^\eta u^* d\eta\right] \qquad (27)$$

Now the momentum equation (1) may be similarly transformed. With the help of Equation (27) and the following identities:

$$\frac{1}{\delta}\frac{\partial \delta}{\partial x^*} = \frac{1}{2}\left(\frac{1}{\lambda}\frac{\partial \lambda}{\partial x^*} - \frac{C\xi^*}{\bar{u}_\infty}\right)$$

$$\frac{1}{\delta}\frac{\partial \delta}{\partial t^*} = \frac{1}{2}\left(\frac{1}{\lambda}\frac{\partial}{\partial t^*} - B\xi^*\right)$$

Equation (1) leads, after some manipulations, to

$$\frac{\partial^2 u^*}{\partial \eta^2} + P_1(\lambda, \eta, t^*)\frac{\partial u^*}{\partial \eta} = P_2(\lambda, \eta, t^*) \qquad (28)$$

where

$$P_1(\lambda,\eta,t^*) = \frac{\lambda}{\xi^*}\left\{ \frac{\eta}{2}\left(\frac{1}{\lambda}\frac{\partial\lambda}{\partial t^*} - B\xi^*\right) + \bar{u}_\infty\left[\left(\frac{1}{\bar{u}_\infty}\frac{\partial\bar{u}_\infty}{\partial x^*} + \frac{1}{2\lambda}\frac{\partial\lambda}{\partial x^*} - \frac{C\xi^*}{2\bar{u}_\infty}\right)\int_0^\eta u^*\,d\eta \right.\right.$$

$$\left.\left. + \frac{\partial\lambda}{\partial x^*}\frac{\partial}{\partial\lambda}\int_0^\eta u^*\,d\eta\right]\right\} \qquad (29)$$

$$P_2(\lambda,\eta,t^*) = \frac{\lambda}{\xi^*}\left\{ \xi^*\left(1 - \frac{A}{4}\right)u^* - \xi^* + \frac{\partial u^*}{\partial t^*} + \frac{\partial\lambda}{\partial t^*}\frac{\partial u^*}{\partial\lambda} + \bar{u}_\infty\frac{\partial\lambda}{\partial x^*}u^*\frac{\partial u^*}{\partial\lambda} \right.$$

$$\left. + \frac{\partial\bar{u}_\infty}{\partial x^*}u^{*2}\right\} \qquad (30)$$

It is noted that this transformation is exact, and the original non-linearities are now included in P_1 and P_2. Consequently, any solution that satisfies Equation (28) is also a solution to the momentum equation (1). In the present improvement technique, Equation (28) is first linearized by evaluating P_1 and P_2 on the basis of the basic integral solution, and then integrated to give refined profiles. The justification comes from the fact that P_1 and P_2 in Equations (29) and (30) only involve profiles and their integrals, and hence the basic integral solution is expected to describe these functions rather accurately. The inaccuracy of the integral solution in predicting profile derivatives, especially the second derivatives, is now significantly reduced by satisfying the governing differential equation (1) or (28) much more closely. Therefore, Equation (28) may now be approximately written as

$$\frac{\partial^2 u^*}{\partial \eta^2} + P_{10} \frac{\partial u^*}{\partial \eta} = P_{20} \tag{31}$$

where P_{10} and P_{20} are P_1 and P_2 evaluated from the basic integral solution, respectively. The corresponding boundary conditions are, for any λ and t^*

$$\eta = 0 \qquad u^* = 0 \qquad \eta \longrightarrow \infty \qquad u^* \longrightarrow 1 \tag{32}$$

In general, solution to the linear equation (31) can be expressed in closed form. However, in view of the composite nature of the assumed profile (10) in the integral solution, it is necessary to integrate Equation (31) separately in the two regions $0 \leq \eta \leq 1$ and $1 \leq \eta \leq \infty$, resulting in

$$\left.\begin{aligned} u_I^* &= C_1 \int_0^\eta e^{-\int_0^\eta P_{10I}\, d\eta}\, d\eta + \int_0^\eta e^{-\int_0^\eta P_{10I}\, d\eta} \left[\int_0^\eta P_{20I}\, e^{\int_0^\eta P_{10I}\, d\eta}\, d\eta \right] d\eta + C_2 \\ u_{II}^* &= C_3 \int_1^\eta e^{-\int_1^\eta P_{10II}\, d\eta}\, d\eta + \int_1^\eta e^{-\int_1^\eta P_{10II}\, d\eta} \left[\int_1^\eta P_{20II}\, e^{\int_1^\eta P_{10II}\, d\eta}\, d\eta \right] d\eta + C_4 \end{aligned}\right\} \tag{33}$$

where the subscript I and II refer to the regions $0 \leq \eta \leq 1$ and $1 \leq \eta \leq \infty$, respectively, and C_1, C_2, C_3 and C_4 are constants of integration, and generally functions of λ and t^*. In order to eliminate these constants, two conditions are required in addition to those in Equations (32), and they are the matching conditions at $\eta = 1$, given by

$$u_I^* = u_{II}^* \qquad \frac{\partial u_I^*}{\partial \eta} = \frac{\partial u_{II}^*}{\partial \eta} \tag{34}$$

Since both P_{10} and P_{20} are continuous throughout the region of η and Equations (34) insure the continuity of

the profile and its first derivative, it is seen that the new profile (33) is at least continuous in its second derivative in view of equation (31). It is pertinent here to mention that, when the exponential profile (12) is assumed in the basic integral solution, the question of this matching in profiles does not arise, and it is only necessary to extend the integrals in (33) to all values of η and evaluate the two constants of integration according to conditions in (32).

As mentioned previously, many improvements of the basic integral procedure have appeared in the literature over the years. Almost without exception, these improvements are justified by comparing results of both the improved solutions and the basic integral solutions with known exact solutions in certain specific cases. One major shortcoming of such justifications is that the accuracy of these improvements is never too well ascertained in cases for which no exact solutions are available. At least for steady-flow theory, this shortcoming has now been corrected by using a simple error criterion, as shown very recently by the present writer [27]. Since there still exists some uncertainty as to whether or not the present formulation of the improvement technique does improve the result based on the integral solution alone for the general unsteady-flow problem, the use of such an error criterion is indeed extremely desirable. It is now to be shown that the development of such an error criterion for the present problem presents no added complexity as

compared to that of the steady-flow theory.

Since the transformation from Equation (1) to Equation (28) is exact, it is clear that the accuracies of the integral solution with and without the present improvement depend largely on how closely Equation (28) is approximated in each case. Consequently, we may define an error quantity ϵ by

$$\epsilon(\lambda,\eta,t^*) = \frac{\partial^2 u^*}{\partial \eta^2} + P_1 \quad \frac{\partial u^*}{\partial \eta} - P_2 \tag{35}$$

which is identically zero for an exact solution. For a given assumed profile in the basic integral solution, deviations from zero for ϵ indicate levels of inaccuracy of the approximate solution. In view of the fact that the error quantity ϵ defined in Equation (35) could have both positive and negative values throughout the entire region of η, it is more convenient to consider a directly related error quantity defined as follows:

$$J(\lambda,t^*) = \frac{\sqrt{R}}{L}\int_0^\infty \epsilon^2 dy = \frac{\delta}{L}\sqrt{R}\int_0^\infty \epsilon^2 d\eta = \frac{\delta\sqrt{R}}{L}\left(\int_0^{'} \epsilon_I^{\,2} d\eta + \int_{'}^{\infty} \epsilon_{II}^2 d\eta\right) \tag{36}$$

where R is characteristic Reynolds number, $u_o L/\nu$. It is noted that this definition of J differs only slightly from that of the steady-flow theory [27] in the inclusion of the boundary-layer thickness δ, and represents an average error of the profile details. To determine the relative degrees of accuracy of the integral solutions with and without the present improvement, it is then only necessary to determine and compare respective J values at different combinations

of λ and t^*. Evidently, smaller values of J correspond to the more accurate profiles. In the actual determination of ϵ, Equation (35) may be used directly for the basic integral solution. For the improvement, a further simplification is possible. Since the improved profile satisfies Equation (31), it may be readily shown that

$$\epsilon = (P_1 - P_{10}) \frac{\partial u^*}{\partial \eta} + (P_{20} - P_2) \tag{37}$$

Finally, it is particularly important to observe that comparisons can only be made of J values based on the same type of assumed profiles used in the basic integral solution. Different types of initially assumed profiles, such as polynomials and exponential functions, inevitably lead to δ's which have entirely different meanings. Since these δ quantities are directly involved in the transformation which eventually leads to Equation (35), meaningful comparisons of the corresponding J values evidently cannot be expected.

The improved integral solution presented in this section specifically deals with the improvement of the local unsteady velocity profiles. In particular, the boundary-layer thickness function δ remains the same as that given by the basic integral solution. Obviously, this is done for the simple reason to keep the calculations at a reasonable level. Nevertheless, it is also conceivable that a similar formulation as that used in the steady-flow theory [27] can be carried out to successively approximate solution to Equation (28) with an iteration scheme based on the integral solution as the zeroth-order approxima-

tion, with the view of possibly obtaining an exact solution. However, in view of the greatly increased complexity of the unsteady-flow problem, such an iteration solution does not seem to be justifiable.

NUMERICAL EXAMPLES

For the purpose of demonstrating the application of the improved integral solution, as well as illustrating the use of the error criterion, several numerical examples have been calculated in detail on an IBM 1620 digital computer. Whenever possible, both assumed profiles, polynomial and exponential function, are used in the basic integral solutions such that range of validity of each of these profiles may be determined. These examples and their results are now described individually.

EXAMPLE 1. Stagnation Hyperbolic Time-Variation Flow

Similarity solutions to the unsteady two-dimensional incompressible boundary-layer equations have been considered by many investigators [7-11]. However, only a few detailed exact velocity profiles are known. Yang [9] has considered the free-stream velocity variation given by

$$\bar{u}_\infty = \frac{x^*}{1 - \alpha t^*} \tag{38}$$

where α is an unsteadiness parameter, positive for acceleration and negative for deceleration. This is known as the stagnation hyperbolic time-variation flow for which a similarity solution exists. The associated ordinary differential equation assumes the following form:

$$f''' + ff'' - (f')^2 + 1 = \alpha\left(\frac{\eta_1}{2} f'' + f' - 1\right) \qquad (39)$$

which is subjected to the boundary conditions

$$f(0) = f'(0) = 0 \qquad f'(\infty) = 1$$

where f' is the velocity profile u^* and prime denotes derivatives with respect to the similarity variable η_1 defined as $y(u_\infty/\nu x)^{1/2}$. Numerical solutions to Equation (39) have also been given by Yang [9] for a wide range of α from -3.0 to +1.6. The available exact velocity profiles, and in particular the profile derivatives provide us with an excellent opportunity to assess the validity of the present improved integral solutions based on both types of assumed profiles.

For this problem, it may be readily shown that $A = 4/(1+\alpha)$, $B = \alpha/(1+\alpha)$ and $C = 0$. Since K is now a constant, dependent only on α, dK/dt^* becomes identically zero. Hence Equation (15) reduces to

$$(1 + \alpha)F_3 + K(\alpha H - 4) = 0 \qquad (40)$$

which immediately yields $\lambda(\alpha)$ and $G(\alpha)$. When these are substituted in Equations (10) and (12), respectively, velocity profiles u_o^* are obtained. This then completes the integral solution. For the improvement solution, functions P_1 and P_2 in Equations (29) and (30) now become

$$P_1 = -\frac{\alpha\lambda}{2(1+\alpha)}\eta + \frac{\lambda}{1+\alpha}\int_0^{\eta} u^* d\eta$$

$$P_2 = \lambda\left[\frac{u^*(u^*+\alpha)}{1+\alpha} - 1\right] \qquad (41)$$

For the exponential function, it is only necessary to replace λ by $(1 + 2G)$. These equations are not only used to evaluate P_{10} and P_{20} from the integral solution, but also to determine P_1 and P_2 from the improved profiles such that the error quantity ϵ, and eventually J may be calculated according to Equations (37) and (36), respectively. Based on both fourth-degree polynomial and the exponential function, the integral solutions with and without the present improvement have been obtained by detailed calculations for α values of 1.6, 1.0, 0, -1.0, -2.4 and -2.8. All corresponding J values have also been evaluated, according to

$$\frac{J}{\sqrt{1-\alpha t^*}} = \sqrt{\frac{\lambda}{1+\alpha}}\left[\int_0^{\infty} \epsilon_I^2 d\eta + \int_{\infty}^{\infty} \epsilon_{II}^2 d\eta\right] \qquad \text{(polynomial)}$$

$$= \sqrt{\frac{1+2G}{1+\alpha}}\int_0^{\infty} \epsilon^2 d\eta \qquad \text{(exponential)}$$

Table 1 shows some results of these calculations in terms of the surface derivatives of the velocity profiles $f''(0)$ and the error quantities $J/\sqrt{1-\alpha t^*}$. Integral solutions based on polynomials only exist up to an α-value of 0.2, while those based on the exponential function does not seem to have an upper limit. Lower limits for both assumed profiles obviously

TABLE 1 - PARTIAL RESULTS FOR EXAMPLE 1

α		Exact Solution	Fourth Degree Polynomial		Exponential Function	
			Integral Solution	Present Solution	Integral Solution	Present Solution
1.6	$f''(0)$	1.6420	———	———	1.6461	1.5739
	$J/\sqrt{1-\alpha t}^*$	0	———	———	7.0302×10^{-6}	1.6476×10^{-4}
1.0	$f''(0)$	1.4986	———	———	1.5161	1.4084
	$J/\sqrt{1-\alpha t}^*$	0	———	———	9.9301×10^{-6}	8.9933×10^{-5}
0	$f''(0)$	1.2326	1.1957	1.2266	1.2868	1.1288
	$J/\sqrt{1-\alpha t}^*$	0	1.3145	1.1489×10^{-1}	8.1646×10^{-4}	1.2302×10^{-4}
-1.0	$f''(0)$	9.2318×10^{-1}	8.7741×10^{-1}	9.1349×10^{-1}	1.0308	8.1656×10^{-1}
	$J/\sqrt{1-\alpha t}^*$	0	7.0772×10^{-1}	1.3241×10^{-2}	3.4085×10^{-3}	8.7016×10^{-5}
-2.4	$f''(0)$	3.8220×10^{-1}	3.7379×10^{-1}	3.6023×10^{-1}	5.8496×10^{-1}	2.6473×10^{-1}
	$J/\sqrt{1-\alpha t}^*$	0	2.1315	1.5224×10^{-2}	2.1034×10^{-2}	9.4199×10^{-4}
-2.8	$f''(0)$	1.9245×10^{-1}	6.9302×10^{-1}	1.4589×10^{-1}	4.1944×10^{-1}	5.8587×10^{-2}
	$J/\sqrt{1-\alpha t}^*$	0	3.1172	6.3247×10^{-2}	3.8226×10^{-2}	2.7680×10^{-3}

correspond to laminar separation. The results shown in Table 1 are very instructive in several respects. Even though the error quantities only indicate an average for the entire profiles and yet $f''(0)$ values refer to only one specific value of η, there is still a good correlation between the two, namely, lower values of the error quantity do correspond to closer agreements with the exact solution. Apparently, these surface profile derivatives are representative of other local profile values as far as accuracy is concerned. For the case of assumed velocity polynomial, it is seen that the present improvement reduces the error in the basic integral solution considerably, indicating a corresponding increase in accuracy of the result. This definitely suggests the validity of the improved solution for general use within the entire range of validity of the basic integral solution based on Pohlhausen's velocity polynomials. However, such a general conclusion cannot be made for the integral solution based on exponential profiles. For negative values of α, the present solution indeed represents improvement. However, when α becomes positive, J-values for the present solution actually exceed that of the basic integral solution, indicating that no improvements are realized in these cases. Consequently, the present solution should not be used. It is emphasized here again that J-values for the two assumed profiles, which are seen to be different by some orders of magnitude, bear no relation to one another, due to entirely different meanings of δ. Therefore, the relative

merits of integral solutions, with and without the present improvement, can only be determined by comparison with the corresponding exact solutions. In this regard, it is clearly seen from Table 1 that within the range of validity of the integral solution based on polynomial profiles, the degrees of accuracy of the improved solution based on polynomials far exceed that based on exponential function. All these observations are further substantiated in Figs. 2-7, incl., which are plots of $f'''(\eta_1)$ based on various solutions calculated for different α-values. These comparisons of $f'''(\eta_1)$, which are directly related to the second profile derivatives, are much more critical than that of $f''(0)$, since it is generally known that by far the major portion of inaccuracy in the basic integral solution occurs in the second profile derivatives and furthermore, these comparisons are made over the complete range of η_1. There is, however, also an indication that the accuracy of the improved solution decreased as laminar separation is approached.

On the basis of the above comparisons in the present problem, which does cover a wide range of free-stream unsteadiness, it is perhaps reasonable to suggest that in a general unsteady problem the improved integral solution based on fourth-degree velocity polynomials is to be used within its entire range of validity, i.e. $12 \geq \lambda \geq -12$. Outside this region for $\lambda > 12$, the results of this problem suggests the use of the basic integral solution with the assumed exponential profile. However, as one of the subsequent examples will show, it is

not always true that in this region the basic integral solution is more accurate than the present solution. Consequently, it is necessary in this region to evaluate both J-values as to determine which is the more accurate. One obvious weakness in the above recommendation is the use of composite solution when λ does exceed 12. However, this is not considered to be too serious, since such λ-values would correspond to extremely large accelerations in the free stream. Further justification of this recommendation can be obtained in considering the following examples.

EXAMPLE 2. <u>The Rayleigh Problem with Step-Change in Free-Stream Velocity</u>

This is the classical problem of an infinite plate moving in a stationary incompressible fluid with a step-change in its velocity. The solution is well known and is given by $u^* = \mathrm{erf}(y/2\sqrt{\nu t})$, relative to the coordinate system fixed on the plate, where erf is the usual error function. Solution to the integral equation in this case is elementary, and is shown in the following:

$$\frac{\delta_2^2}{\nu t} = \left(\frac{2F_2}{H}\right)_{K=0} \tag{42}$$

The integral solution is then obtained by substituting the above equation in the profile equation (10) and (12). The corresponding error criterion is simply

$$\frac{J_o}{t^*} = \frac{4}{\beta^2} \int_0^\infty \epsilon^2 d\eta \tag{43}$$

where $\beta = \left[(2H/\bar{F}_2)^{1/2}\ (\delta_2/\delta)\right]_{K=0}$. The improved integral solution for this problem is equally elementary. Functions $\bar{P}_1$ and $\bar{P}_2$ in Equation (29) and (30) reduce to

$$\bar{P}_{10} = \frac{2}{\beta_2}\eta \qquad\qquad \bar{P}_{20} = 0 \tag{44}$$

respectively. Solution to Equation (31), satisfying the boundary conditions in (32), is simply $u^* = \text{erf}(\eta/\beta)$. However, since it can be shown readily that η_2 defined as $y/2\sqrt{\nu t}$ is related to η by $\eta = \eta_2\beta$, the solution now becomes

$$u^* = \text{erf}(\eta_2) \tag{45}$$

which is obviously identically to the exact solution. Thus, it is seen that for this problem, the improved procedure leads to exact solution, regardless of the type of profiles used in the integral solution. The calculated J-values, as well as the surface profile derivatives, are shown in Table 2.

EXAMPLE 3. The Rayleigh Problem with Constant Acceleration

This problem is similar to the previous one except that the free-stream velocity undergoes constant acceleration from rest. Exact solution to this problem is again known [6], and is given by

$$u^* = 1 + \frac{2}{\sqrt{\pi}}\ \eta_2 e^{-\eta_2^2} - (1 + 2\eta_2^2)\ \left[1 - \text{erf}(\eta_2)\right] \tag{46}$$

The solution to the integral equation (16) has been given by Yang [25], and may be written as

TABLE 2 - RESULTS FOR EXAMPLE 2

		$\left(\frac{du^*}{d\bar{\eta}_2}\right)_w$	$\frac{\bar{J}}{t^*}$
Integral Solution	polynomial	1.0954	3.4249
	exponential	1.2247	4.6340×10^{-2}
Improved Solution		1.1284	0
Exact Solution		1.1284	0

$$\frac{\delta_2^2}{\nu t} = \frac{2}{3}\frac{\bar{F}_2(K_o)}{H(K_o)} \tag{47}$$

where K_o is a constant satisfying Equation (18). Since the corresponding value of λ exceeds +12, only the result based on exponential function can be considered. Thus, Equation (18) leads to a G-value of -1/3. The error criterion for the integral solution is now

$$\frac{J}{\sqrt{t^*}} = \frac{1}{\sqrt{3}}\int_0^\infty \epsilon^2 d\eta \tag{48}$$

Now for the improved solution, Equations (29) and (30) reduce respectively to

$$P_{10} = \frac{\eta}{6} \qquad P_{20} = \frac{1}{3}(u_o^* - 1) \tag{49}$$

The integrals in the solution to Equation (31) have been evaluated numerically, yielding the new profile $u^* = u^*(\eta)$. Finally, this may be transformed into the physical plane by

$$\eta = \sqrt{\frac{6H(K_o)}{F_2(K_o)}} \qquad \left(\frac{\delta_2}{\delta}\right)_{K_o} \qquad \eta_2$$

Since P_1 based on the newly obtained profile is identical to P_{10}, the error quantity ε now simply becomes $(u_o^* - u^*)/3$ in view of Equation (37), and the corresponding J-value has also been determined from Equation (48). The comparison of J-values and surface profile derivatives is shown in Table 3, and that of the second profile derivatives, in Fig. 8. It is seen that the present solution is much more accurate than the basic integral solution, a result which is contrary to that obtained in the first example. It is therefore clear that in this region of application for $\lambda > 12$, it is necessary to compute the error quantities for both the integral solutions with and without the present improvement, such that the more accurate result can be determined.

TABLE 3 - RESULTS FOR EXAMPLE 3

	$\left(\frac{du^*}{d\eta_2}\right)_w$	$\frac{J}{\sqrt{t^*}}$
Integral Solution (exponential)	2.3094	0.4459×10^{-3}
Present Solution	2.2662	0.7682×10^{-4}
Exact Solution	2.2568	0

EXAMPLE 4. Unsteady Flow over Semi-Infinite Plate with Constant Acceleration from Rest

This represents one of the problems in which the leading edge plays a very important role in the solutions. These problems have been systematically studied in the literature [12-14]. In particular, this very problem is covered in the series solutions of Cheng [13], and Cheng and Elliott [14], which are, however, only valid for flat plates and free-stream velocity starting from rest. In this numerical example, attention is to be placed only in the region close to the leading edge, since it is in this region that the basic integral equation (6) for this problem reduces to Equation (17) exactly, which is now to be solved in terms of the boundary condition $K(0) = 0$. The solution may be expressed in terms of integrals, as follows:

$$P = e^{-\int_0^K \frac{2F_1}{2F_2 - 3KH} dK} \int_0^K \frac{e^{\int_0^K \frac{2F_1}{2F_2 - 3KH} dk}}{2F_2 - 3KH} dK \qquad (50)$$

which immediately yields either $\lambda = \lambda(P)$ or $G = G(P)$, depending on the assumed profiles, which then leads to the profile details according to the integral solution. For the improved solution, functions P_1 and P_2 now become

$$P_1 = \frac{\eta}{2}(\lambda - 2P\lambda') + \frac{\lambda'}{2}\int_0^\eta u^* d\eta + \lambda\lambda' \frac{\partial}{\partial\lambda}\int_0^\eta u^* d\eta$$

$$P_\lambda = \lambda\left[(u^* - 2P)\lambda' \frac{\partial u^*}{\partial\lambda} + u^* - 1\right] \qquad (51)$$

respectively, where prime denotes derivatives with respect to P. Equations (51) are explicitly written for the case where velocity polynomials are considered. However, they are equally valid for exponential functions, provided again that λ is replaced by $(1 + 2G)$. When Equations (51) are evaluated from the integral solution u_o^* and the following identities are utilized:

$$\lambda' = \frac{2F_2 - 3KH}{1 - 2PF_1} \frac{1}{\left(\frac{37}{315} - \frac{\lambda}{945} - \frac{\lambda^2}{9072}\right)\left(\frac{37}{315} - \frac{\lambda}{315} - \frac{5\lambda^2}{9072}\right)}$$

$$G' = \frac{2(1 - 2G)(1 + 3G)}{G(8 + 5G - 24P)}$$

where prime again refers to derivatives with respect to P, Equation (31) is then solved in terms of integrals which in turn are evaluated numerically. This calculation has been carried out for both profiles for a range of P in the neighborhood of P = 0. The J-values for the basic integral solutions can be readily evaluated from Equation (36). However, calculation of that of the corresponding improved solutions gives rise to a slight complication which needs special treatment. This is a characteristic to all general problems with non-similar profiles, as already pointed out by Yang [27].

In order to evaluate the error quantity ϵ from Equation (37), it is necessary first to determine functions P_1 and P_2 from the improved profiles. However, in view of Equations (51), the distribution of $\partial u^*/\partial P$ at all values of η must be known. Even though it could possibly be evaluated by numerical differentiation from improved profiles at various P-values, such an evaluation would be extremely awkward, and it is highly desirable to be able to determine this distribution at any particular value of P. This can be accomplished by the following scheme. Differentiating Equation (31) with respect to P yields

$$\frac{\partial^2}{\partial\eta^2}\left(\frac{\partial u^*}{\partial P}\right) + P_{10}\frac{\partial}{\partial\eta}\left(\frac{\partial u^*}{\partial P}\right) = \frac{\partial P_{20}}{\partial P} - \frac{\partial P_{10}}{\partial P}\frac{\partial u^*}{\partial\eta} \qquad (52)$$

which is subjected to the boundary conditions

$$\eta = 0 \quad \frac{\partial u^*}{\partial P} = 0 \qquad\qquad \eta \to \infty \quad \frac{\partial u^*}{\partial P} \to 0 \qquad (53)$$

Now Equation (52) may be solved in an identical way as that for Equation (31), resulting in $\partial u^*/\partial P$. Thus, this determination is frozen at any P-value.

The calculated results for this problem are shown in Figs. 9 and 10, together with the series solution of Cheng [13], which is believed to be accurate in this problem, in view of the nature of his solution. More specifically, Fig. 9 shows the variation of local skin-friction coefficient $c_f = \tau_w/(1/2\rho u_o^2)$ with P and Fig. 10, the variation of the

J-values. It is noted that all curves in Fig. 10 go through $J = 0$ at $P = 0$, since there is no motion then and accordingly, $\delta = 0$, yielding $J = 0$ in view of Equation (36). These results again show the good correlation between the calculated J-values and the relative accuracies of the integral solutions with and without the present improvement. This represents further evidence of the validity of the use of the error criterion. Moreover, it is also seen that the improved integral solution based on polynomials is much more accurate than that based on exponential functions. Since in this problem values of λ are all under the limit of 12, this result agrees well with that of the first example.

EXAMPLE 5. Transient Boundary-Layer Development on a Semi-Infinite Plate

This problem deals with the effect of step-wise change in free-stream velocity on the development of unsteady boundary layer on a semi-infinite plate which is originally in steady motion. The step-wise change may represent either acceleration or deceleration. The integral solution to this problem, based on the method of characteristics, has already been presented previously, and is shown in Equation (23). Only the transient solution is considered here, since the steady-state solution has already been treated in the literature [26]. For this problem, functions P_1 and P_2 are given by

$$\left.\begin{aligned} P_1 &= \left\{ F_2 \left(\frac{\delta}{\delta_2}\right)^2 \left[\frac{\eta}{H}\left(1 - \frac{\bar{u}_\infty}{\bar{u}_{\infty 1}}\right) + \frac{\bar{u}_\infty}{\bar{u}_{\infty 1}} \int_0^\eta u^* d\eta \right] \right\}_{K=0} \\ P_2 &= 0 \end{aligned}\right\} \qquad (54)$$

Detailed numerical calculations of the integral solutions with and without the present improvement, based on both assumed profiles, have been carried out for two values of $\bar{u}_\infty/\bar{u}_{\infty i}$, namely, 2.0 and 0.5, and several combinations of x^* and t^*. In addition, all pertinent values of J have also been determined. Since no exact solution is available to this problem in the literature, no comparison can be made and only some representative results are presented. Table 4 shows the calculated results for several specific combinations of x^* and t^*, and some typical velocity profiles are described in Fig. 11 to 14, incl. These results again clearly indicate the validity of the improved solution. Finally, it is to be noted that in a normal application to the present problem, it is not necessary to obtain the integral solutions based on exponential functions, since here λ is identically zero, which is well within the range of validity of the integral solutions based on polynomials.

EXAMPLE 6. Unsteady Flow over a Circular Cylinder

This last example treats a general unsteady boundary-layer problem of flow over a circular cylinder. The free-stream velocity distribution is written as

$$\bar{u}_\infty = \phi(x^*)g(t^*) \tag{55}$$

where

$$\phi(x^*) = 3.6314x^* - 2.1709x^{*3} - 1.5144x^{*5}$$

$$g(t^*) = 1 - t^* + t^{*2} \qquad t^* \geq 0$$

$$= | \qquad t^* < 0$$

TABLE 4 - RESULTS FOR PROBLEM 5

	$\bar{u}_{c_3}/\bar{u}_{\infty 1}$	x^*	t^*	z^*	J_0	J_1
	2.0	0.3	0.1149	0.1198	4.4088	5.3325×10^{-2}
			0.3448	0.0775	3.5465	4.2895×10^{-2}
		0.6	0.2299	0.2396	6.2350	7.5413×10^{-2}
			0.6896	0.1550	5.0155	6.0662×10^{-2}
		0.9	0.3448	0.3594	7.6363	9.2362×10^{-2}
			1.0344	0.2326	6.1427	7.4296×10^{-2}
	0.5	0.3	0.4597	0.1832	0.5475	8.0525×10^{-4}
			1.3792	0.2678	0.6619	9.7350×10^{-4}
		0.6	0.9195	0.3665	0.7743	1.1388×10^{-3}
			2.7584	0.5356	0.9361	1.1377×10^{-3}
		0.9	1.3792	0.5497	0.9483	1.3947×10^{-3}
			4.1376	0.8034	1.1464	1.6861×10^{-3}
	2.0	0.3	0.0982	0.1753	3.2546×10^{-2}	1.5309×10^{-3}
			0.2945	0.1134	2.6180×10^{-2}	1.2314×10^{-3}
		0.6	0.1964	0.3506	4.6027×10^{-2}	2.1650×10^{-3}
			0.5891	0.2269	3.7024×10^{-2}	1.7415×10^{-3}
		0.9	0.2945	0.5259	5.6372×10^{-2}	2.6515×10^{-3}
			0.8836	0.3403	4.5345×10^{-2}	2.1329×10^{-3}
	0.5	0.3	0.3927	0.2681	1.0840×10^{-2}	1.1325×10^{-5}
			1.1782	0.3919	1.3105×10^{-2}	1.3692×10^{-5}
		0.6	0.7855	0.5362	1.5330×10^{-2}	1.6017×10^{-5}
			2.3564	0.7838	1.8533×10^{-2}	1.9363×10^{-5}
		0.9	1.1782	0.8044	1.8775×10^{-2}	1.9616×10^{-5}
			3.5345	1.1756	2.2698×10^{-2}	2.3715×10^{-5}

where $\phi(x^*)$ is the steady free-stream velocity distribution over a circular cylinder as given by Heimenz [32]. Even though this variation is now known not to be too accurate, it, nevertheless, serves the present purpose. The chosen time variation is one involving initially steady motion, then deceleration, and finally followed by an acceleration. The general calculation procedure described previously for a general unsteady problem to obtain solution to the integral equation is here used. All integrations have been carried out by the usual fourth-order Runge-Kutta routine. The result of this solution based on polynomial profiles only is shown in Fig. 15. For this problem Equations (29) and (30) are used directly, since no simplification is possible. When the integral solution $u_o^*(\lambda,\eta)$ is substituted into Equations (33), improved profile at any combination of x^* and t^* is easily obtained. To calculate the error quantity of the improved solution, it is now necessary to first evaluate $\partial u^*/\partial\lambda$ and $\partial u^*/\partial t^*$ from the improved profile. This is again done by first differentiating Equation (31) with respect to λ and t^*, and then following the same scheme as that indicated in Equation (52). Some results are shown in Table 5 and Fig. 16. Here again the improved accuracy in the present solution may be noted.

TABLE 5 - RESULTS FOR PROBLEM 6

t^*	x^*	J_o	J_1
0.10000	0.20000	0.45949	0.14488
0.30000	0.10000	0.33981	0.04810
0.20000	0.10000	0.38370	0.04412
0.10000	0.40000	0.43801	0.11147
0.20000	0.40000	0.36692	0.01324
0.30000	0.30000	0.33221	0.04215
0.40000	0.20000	0.28828	0.09272
0.40000	0.40000	0.26568	0.05756
0.50000	0.30000	0.22076	0.18338
0.50000	0.40000	0.20654	0.12395

CONCLUDING REMARKS

In this report an improved integral procedure, based on two types of assumed profiles, is proposed to calculate the behavior of unsteady laminar boundary layers over arbitrary cylinders with arbitrarily prescribed unsteadiness in the free stream. Also introduced is a simple error criterion by which the validity of the improved solution can be readily determined. In view of results from the numerical examples, this error criterion correlates extremely well with the inaccuracy of the approximate solutions on the basis of comparing results with that from the exact solutions. Furthermore, the critical comparisons in the second profile derivatives from the integral solutions with and without the present improvement technique and from the exact solutions in the first four numerical examples have definitely indicated the high degree of accuracy attainable in the present solution. As mentioned previously, such accuracy is necessary for hydrodynamic stability considerations. Consequently, the following recommendation has evolved in the present study. For any general unsteady-flow problem, the improved integral solution based on the fourth-degree polynomial as the assumed profiles in the basic integral solution should be used within the entire range of validity of this basic integral solution. High degree of accuracy can be expected, except possibly in the immediate neighborhood of the point of laminar separation. Outside of this range, both integral solutions based on assumed exponential functions should be utilized. The final solution here, being either the basic integral solution or the improved solution, is evidently the one with lower magnitude of the error quantity J.

REFERENCES

1. Stewartson, K., "The Theory of Unsteady Laminar Boundary Layers," Advances in Applied Mechanics, vol. 6, Academic Press, New York (1960).

2. Hasimoto, H., "Boundary Layer Growth on a Flat Plate with Suction or Injection," Journal of Physical Society of Japan, vol. 12, pp. 68-72 (1957).

3. Yang, K. T., "Unsteady Laminar Compressible Boundary Layers on an Infinite Plate with Suction or Injection," Journal of the Aero/Space Sciences, vol. 26, no. 10, pp. 654-662 (1959).

4. Schetz, J. A. and Zeiberg, S. L., "On Unsteady Laminar Flow with Mass Transfer," paper presented at the 4th U. S. National Congress of Applied Mechanics, University of California, Berkeley, California, June 18-21 (1962).

5. Watson, J., "A Solution of the Navier-Stokes Equations Illustrating the Response of a Laminar Boundary Layer to a Given Change in the External Stream Velocity," Quarterly Journal of Mechanics and Applied Mathematics, vol. 11, pp. 302-325 (1958).

6. Schlichting, H., "Boundary Layer Theory," Translated by J. Kestin, fourth edition, McGraw-Hill Book Co., Inc., New York (1960).

7. Schuh, H., "Über die ähnlichen Losungen der instationären laminaren Grenzschichtgleichung in inkompressibler Strömung," Festschrift "50 Jahr Grenzchichtforschung," herausgeg von Görtler und W. Tollmein, Verlag Vieweg, Braunschweig, Germany, pp. 147-152 (1955).

8. Geis, T., "Bemerkung zu den Ähnlichen instationaren laminaren Grenzchichtstromungen," Zeitschrift fur ungewandte Mathematik und Mechanik, vol. 36, pp. 396-398 (1956).

9. Yang, K. T., "Unsteady Laminar Boundary Layers in an Incompressible Stagnation Flow," Journal of Applied Mechanics, vol. 25, Trans. ASME, vol. 80, pp. 421-427 (1958).

10. Hassan, H. A., "On Unsteady Laminar Boundary Layers," Journal of Fluid Mechanics, vol. 9, pp. 300-304 (1960).

11. Hayasi, N., "On Similar Solutions of the Unsteady Quasi-Two-Dimensional Incompressible Laminar Boundary-Layer Equation," Journal of the Physical Society of Japan, vol. 16, no. 11, pp. 2316-2329 (1961).

12. Stewartson, K., "On the Impulsive Motion of a Flat Plate in a Viscous Fluid," Quarterly of Applied Mathematics and Mechanics, vol. 4, pp. 182-198 (1951).

13. Cheng, S. I., "Some Aspects of Unsteady Laminar Boundary Layer Flows," Quarterly of Applied Mathematics, vol. 14, pp. 337-352 (1956-7).

14. Cheng, S. I. and Elliott, D., "The Unsteady Laminar Boundary Layer on a Flat Plate," preprints of papers, Heat Transfer and Fluid Mechanics, Institute, Stanford University, Stanford, California, pp. 221-238 (1956).

15. Lighthill, M. J., "The Response of Laminar Skin Friction and Heat Transfer to Fluctuations in the Stream Velocity," Proceedings of the Royal Society of London, England, series A, vol. 224, pp. 1-23 (1954).

16. Stuart, J. T., "A Solution of the Navier-Stokes Equations Illustrating the Response of Skin Friction and Temperature of an Infinite Plate Thermometer to Fluctuations in the Stream Velocity," Proceedings of Royal Society, Series A, vol. 221, pp. 116-130 (1955).

17. Glauert, M. B., "The Laminar Boundary Layer on Oscillating Plates and Cylinders," Journal of Fluid Mechanics, vol. 1, pp. 97-110 (1956).

18. Rott, N., "Unsteady Viscous Flow in the Vicinity of a Stagnation Point," Quarterly of Applied Mathematics, vol. 13, pp. 444-451 (1956).

19. Rott, N. and Rosenzweig, M. L., "On the Response of the Laminar Boundary Layer to Small Fluctuations of the Free-Stream Velocity," Journal of Aero/Space Sciences, vol. 27, pp. 741-747 (1960).

20. Lin, C. C., "Motion in the Boundary Layer with a Rapidly Oscillating External Flow," Proceedings of the 9th International Congress of Applied Mechanics, Brussels, vol. 4,pp. 155-167 (1957).

21. Hill, P. G. and Stenning, A. H., "Laminar Boundary Layers in Oscillating Flow," Journal of Basic Engineering, Trans. ASME, vol. 82, Series D, no. 3, pp. 593-608 (1960).

22. Carrier, G. F. and Di Prima, R. D., "On the Unsteady Motion of a viscous Fluid Past a Semi-Infinite Flat Plate," Quarterly of Applied Mathematics, vol. 35, pp. 359-383, (1957).

23. Moore, F. K., "Unsteady Laminar Boundary-Layer Flow," NACA TN 2471 (1951).

24. Schuh, H., "Calculation of Unsteady Boundary Layers in Two-Dimensional Laminar Flow," Zeitschrift fur Flugwissenschaften, vol. 1, pp. 122-131 (1953).

25. Yang, K. T., "Unsteady Laminar Boundary Layers over an Arbitrary Cylinder with Heat Transfer in an Incompressible Flow". Journal of Applied Mechanics, vol. 26, Trans. ASME, vol. 81, Series E, pp. 171-178 (1959).

26. Yang, K. T., "An Improved Integral Procedure for Compressible Laminar Boundary-Layer Analysis," Journal of Applied Mechanics, vol. 28, Trans. ASME, Series E, vol. 83, pp. 9-20 (1961).

27. Yang, K. T., "On an Improved Karman-Pohlhausen's Integral Procedure and a Related Error Criterion," paper presented at the 4th U. S. National Congress of Applied Mechanics, University of California, Berkeley, California, June 18-21 (1962).

28. Schlichting, H., "Boundary Layer on Flat Plate under Condition of Suction and Air Injection," Luftfahrtforschung, vol. 19, no. 9, pp. 293-301 (1942).

29. Lew, H. G., "On the Compressible Boundary Layer over a Flat Plate with Uniform Suction," Reissner Anniversary Volume, J. W. Edwards, Ann Arbor, Michigan, pp. 42-60 (1949).

30. Yang, K. T., "Calculation of Unsteady Heat Conduction in Single-Layer and Composite Finite Slabs with and without Property Variations by an Improved Integral Procedure," paper presented at the Second International Heat Transfer Conference, Boulder, Colorado, Aug. 28-Sept. 1 (1961).

31. Yang, K. T., "Laminar Forced Convection of Liquids in Tubes with Variable Viscosity," Journal of Heat Transfer, Trans. ASME, vol. 84, Series C, no. 4, pp. 353-362 (1962).

32. Hiemenz, K., "Die Grenzschicht an einem in den gleichformigen Flussigkeitsstrom eingetauchten geraden Kreiszylinder," Journal of Dingl. Polytechn., vol. 326, p. 32 (1911).

CAPTION OF FIGURES

1. Grid System for Calculation in General Unsteady Problem
2. Comparison of $f'''(\eta_1)$ for $\alpha = 1.6$, Example 1
3. Comparison of $f'''(\eta_1)$ for $\alpha = 1.0$, Example 1
4. Comparison of $f'''(\eta_1)$ for $\alpha = 0$, Example 1
5. Comparison of $f'''(\eta_1)$ for $\alpha = -1.0$, Example 1
6. Comparison of $f'''(\eta_1)$ for $\alpha = -2.4$, Example 1
7. Comparison of $f'''(\eta_1)$ for $\alpha = -2.8$, Example 1
8. Comparison of Second Profile Derivatives, Example 3
9. Comparison of Local Skin-Friction Coefficients, Example 4
10. Comparison of Local Error Quantities, Example 4
11. Typical Velocity Profiles for $\bar{u}_\infty/\bar{u}_{\infty i} = 2.0$ Based on Polynomial, Example 5
12. Typical Velocity Profiles for $\bar{u}_\infty/\bar{u}_{\infty i} = 0.5$ Based on Polynomial, Example 5
13. Typical Velocity Profiles for $\bar{u}_\infty/\bar{u}_{\infty i} = 2.0$ Based on Exponential Function, Example 5
14. Typical Velocity Profiles for $\bar{u}_\infty/\bar{u}_{\infty i} = 0.5$ Based on Exponential Function, Example 5
15. Integral Solution $\lambda = \lambda(x^*, t^*)$, Example 6
16. Typical Velocity Profiles, Example 6

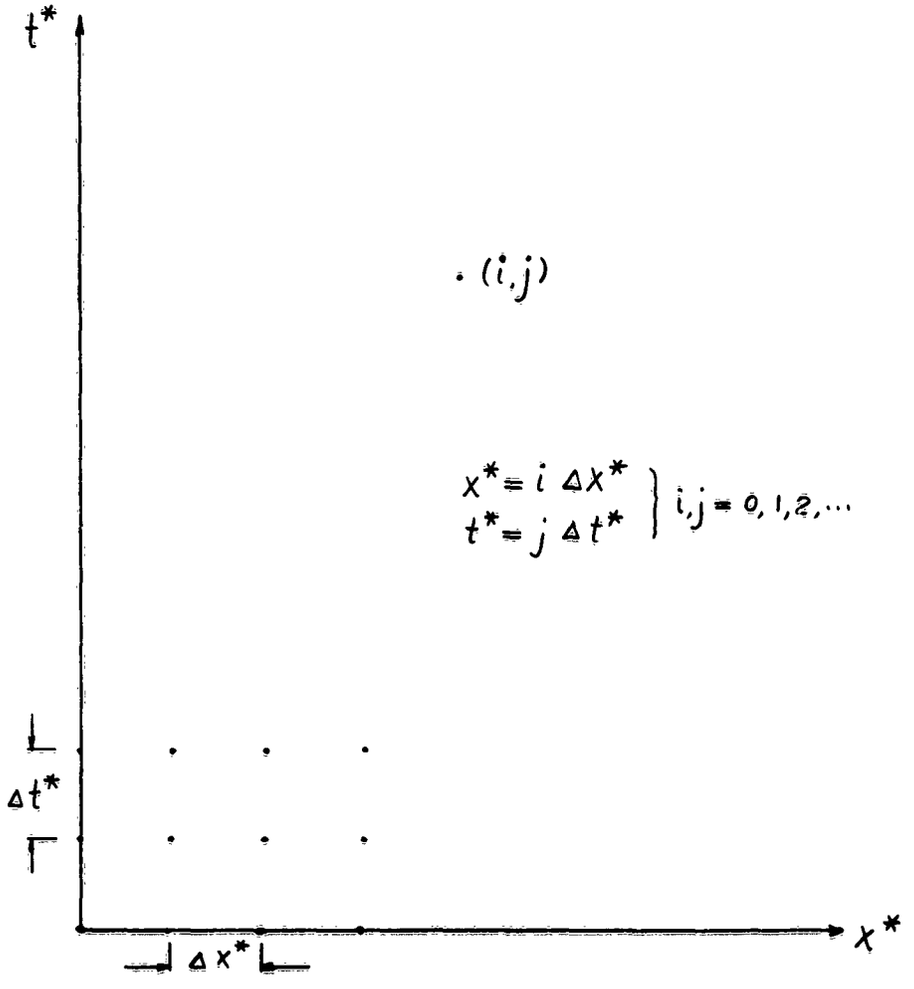

FIG. 1.

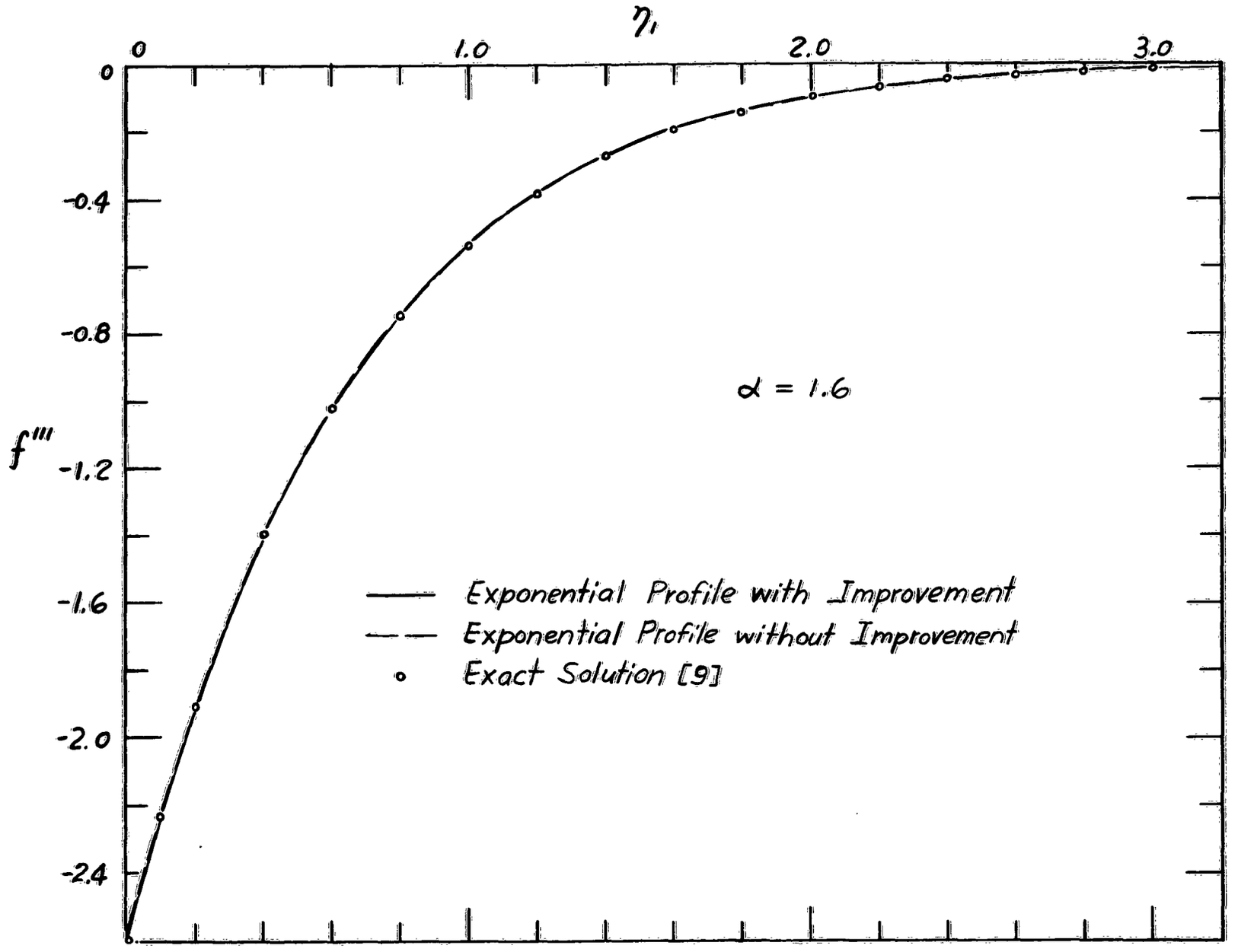
η
0
1.0
2.0
3.0
0
-0.4
-0.8
-1.2
-1.6
-2.0
-2.4
f'''
α = 1.6
Exponential Profile with Improvement
Exponential Profile without Improvement
Exact Solution [9]

FIG. 2.

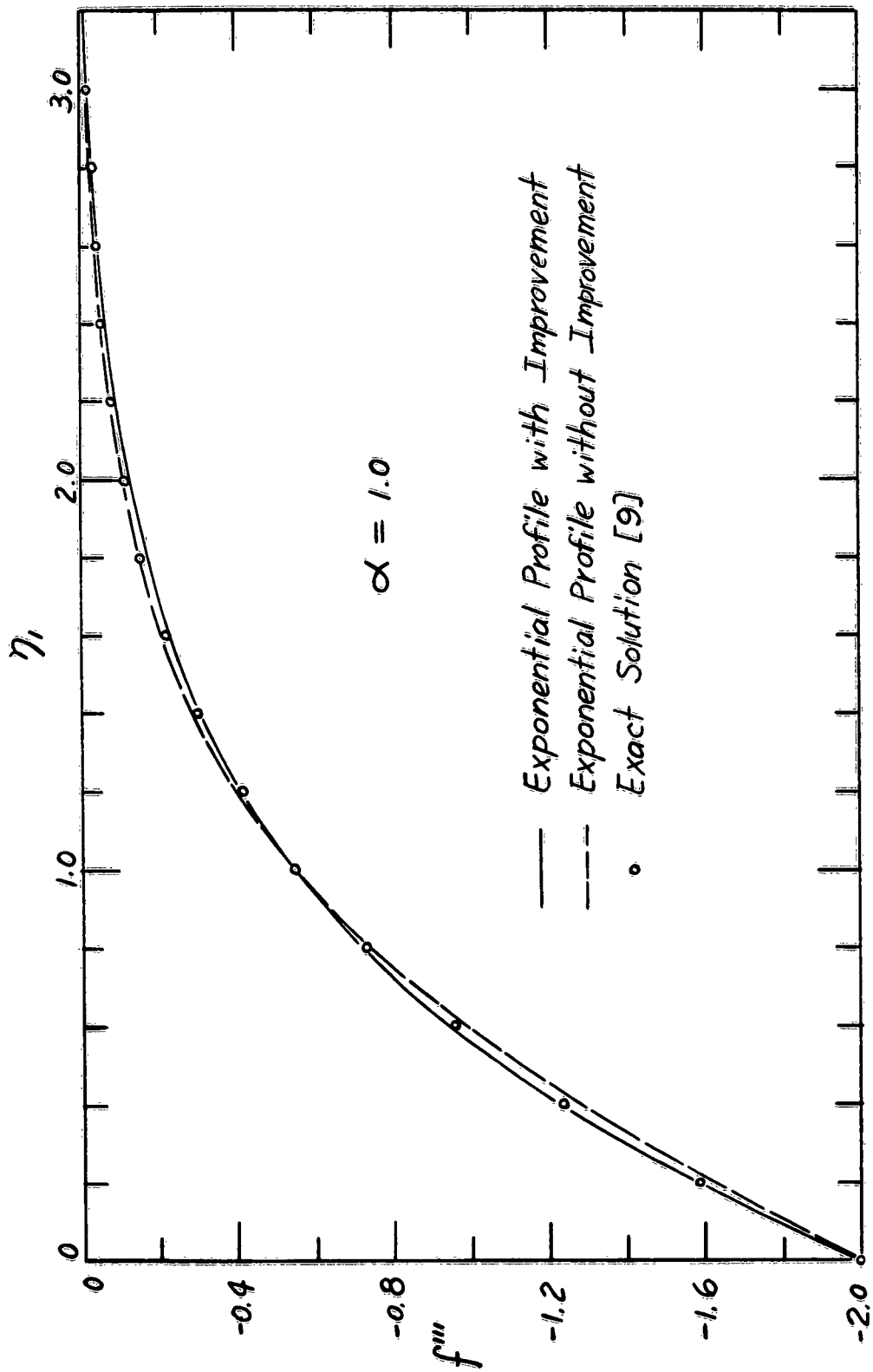
η
0
1.0
2.0
3.0
f'''
0
-0.4
-0.8
-1.2
-1.6
-2.0
α = 1.0
Exponential Profile with Improvement
Exponential Profile without Improvement
Exact Solution [9]

FIG. 3

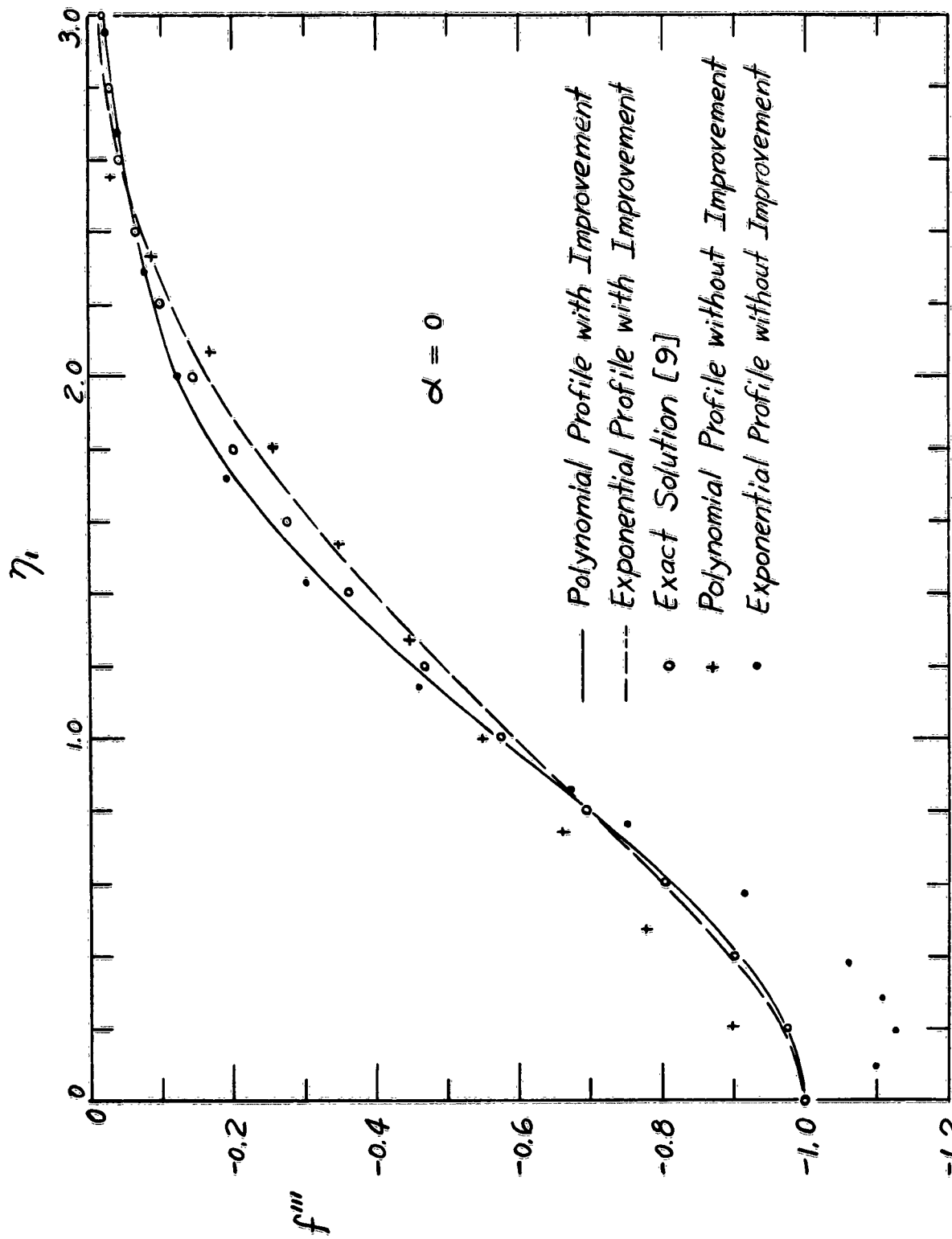
η
f'''
0
1.0
2.0
3.0
-0.2
-0.4
-0.6
-0.8
-1.0
-1.2
α = 0
Polynomial Profile with Improvement
Exponential Profile with Improvement
Exact Solution [9]
Polynomial Profile without Improvement
Exponential Profile without Improvement

FIG. 4.

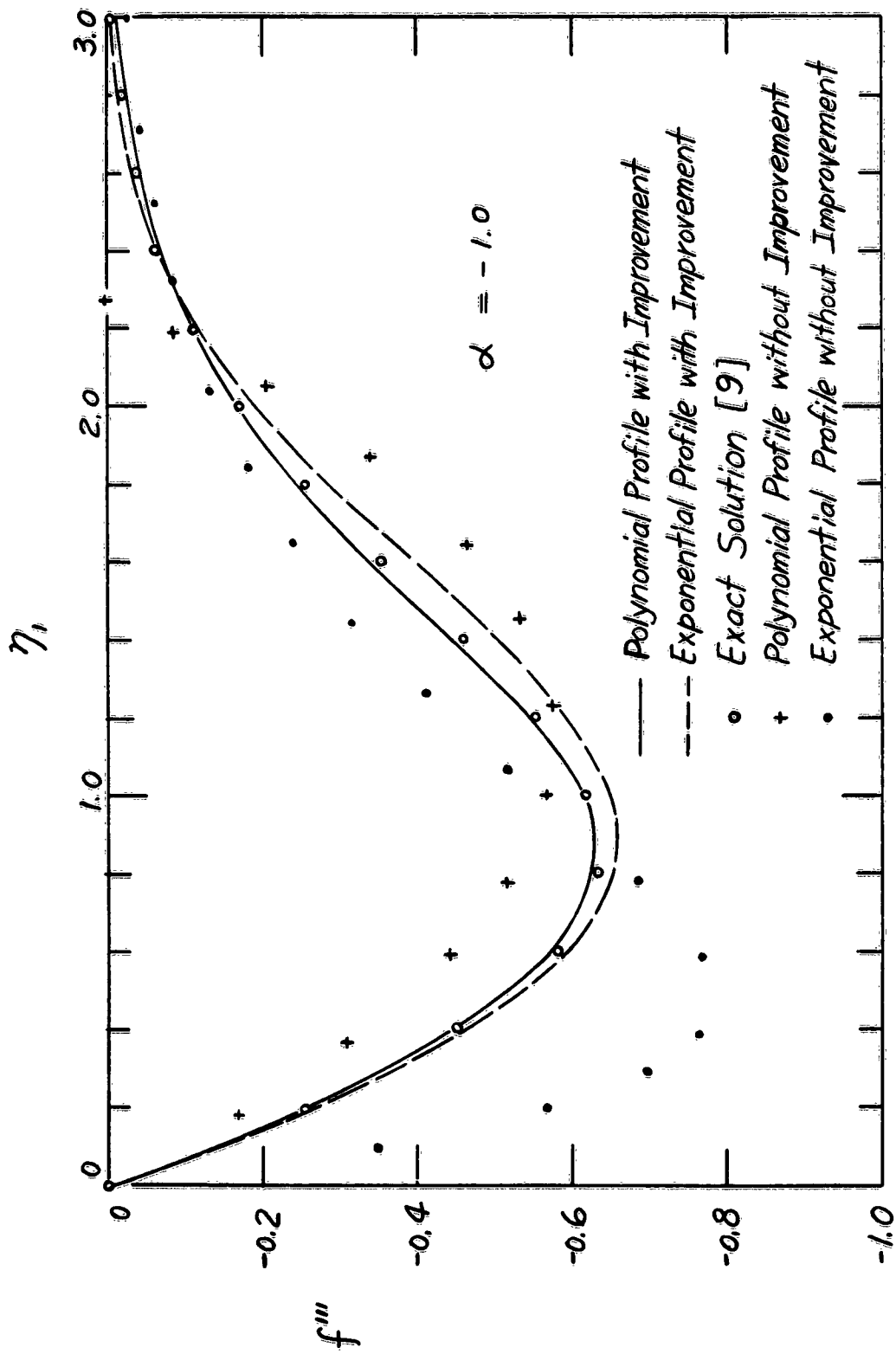
η
f'''
0
1.0
2.0
3.0
-0.2
-0.4
-0.6
-0.8
-1.0
α = - 1.0
Polynomial Profile with Improvement
Exponential Profile with Improvement
Exact Solution [9]
Polynomial Profile without Improvement
Exponential Profile without Improvement

FIG. 5.

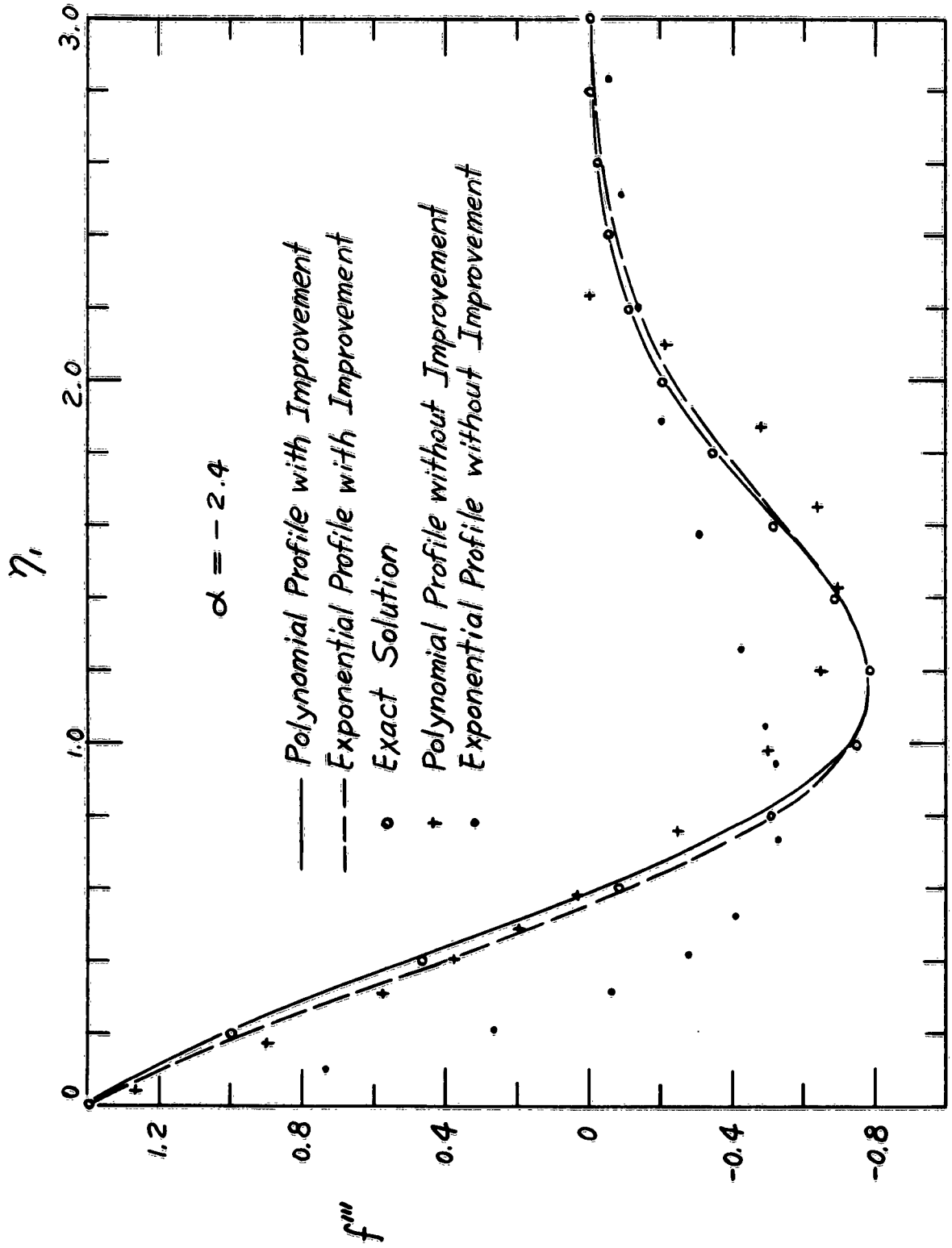
η
f'''
α = −2.4
Polynomial Profile with Improvement
Exponential Profile with Improvement
Exact Solution
Polynomial Profile without Improvement
Exponential Profile without Improvement
0
1.0
2.0
3.0
1.2
0.8
0.4
0
-0.4
-0.8

FIG. 6.

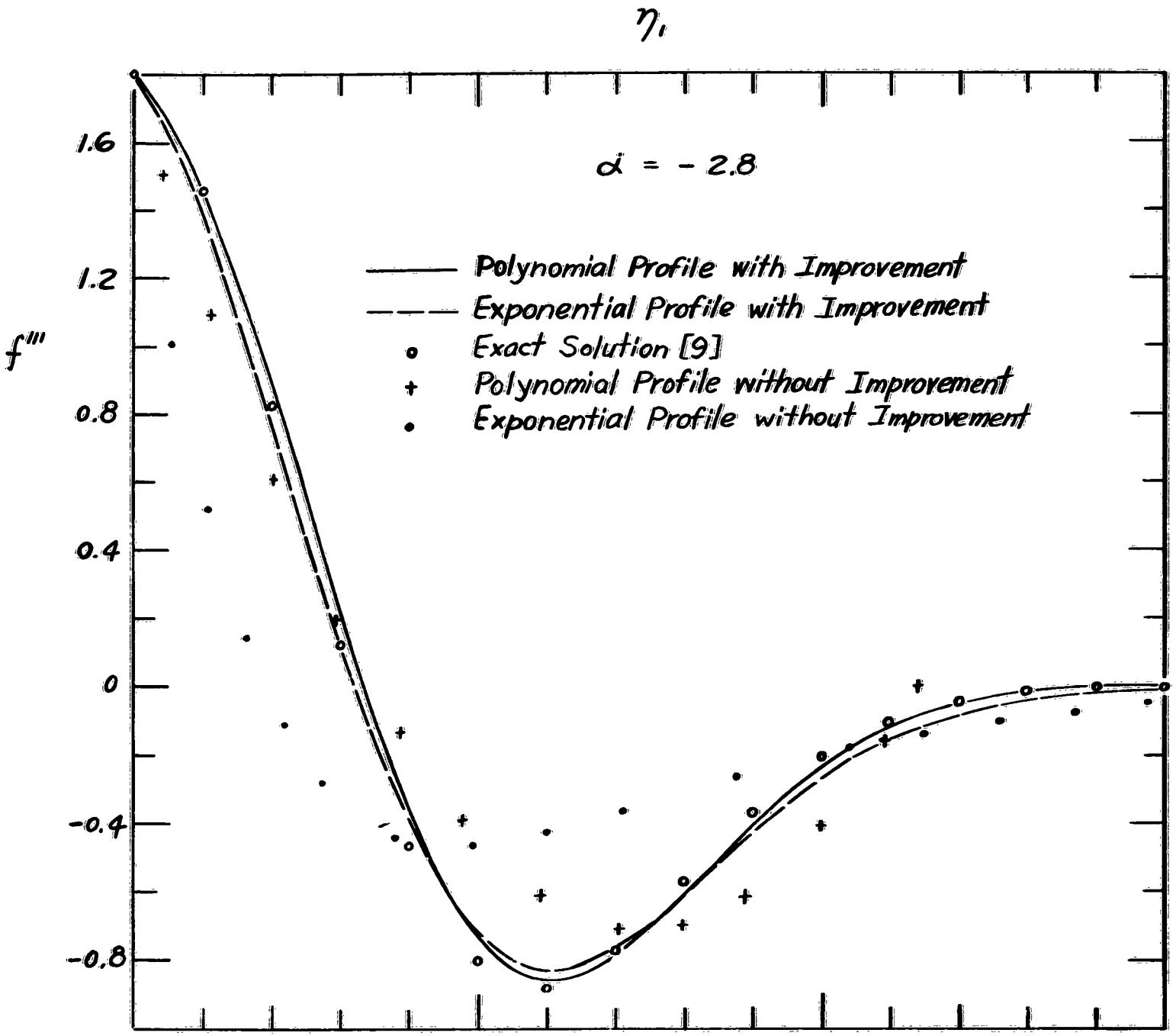
η
f'''
1.6
1.2
0.8
0.4
0
-0.4
-0.8
α = - 2.8
Polynomial Profile with Improvement
Exponential Profile with Improvement
Exact Solution [9]
Polynomial Profile without Improvement
Exponential Profile without Improvement

FIG. 7.

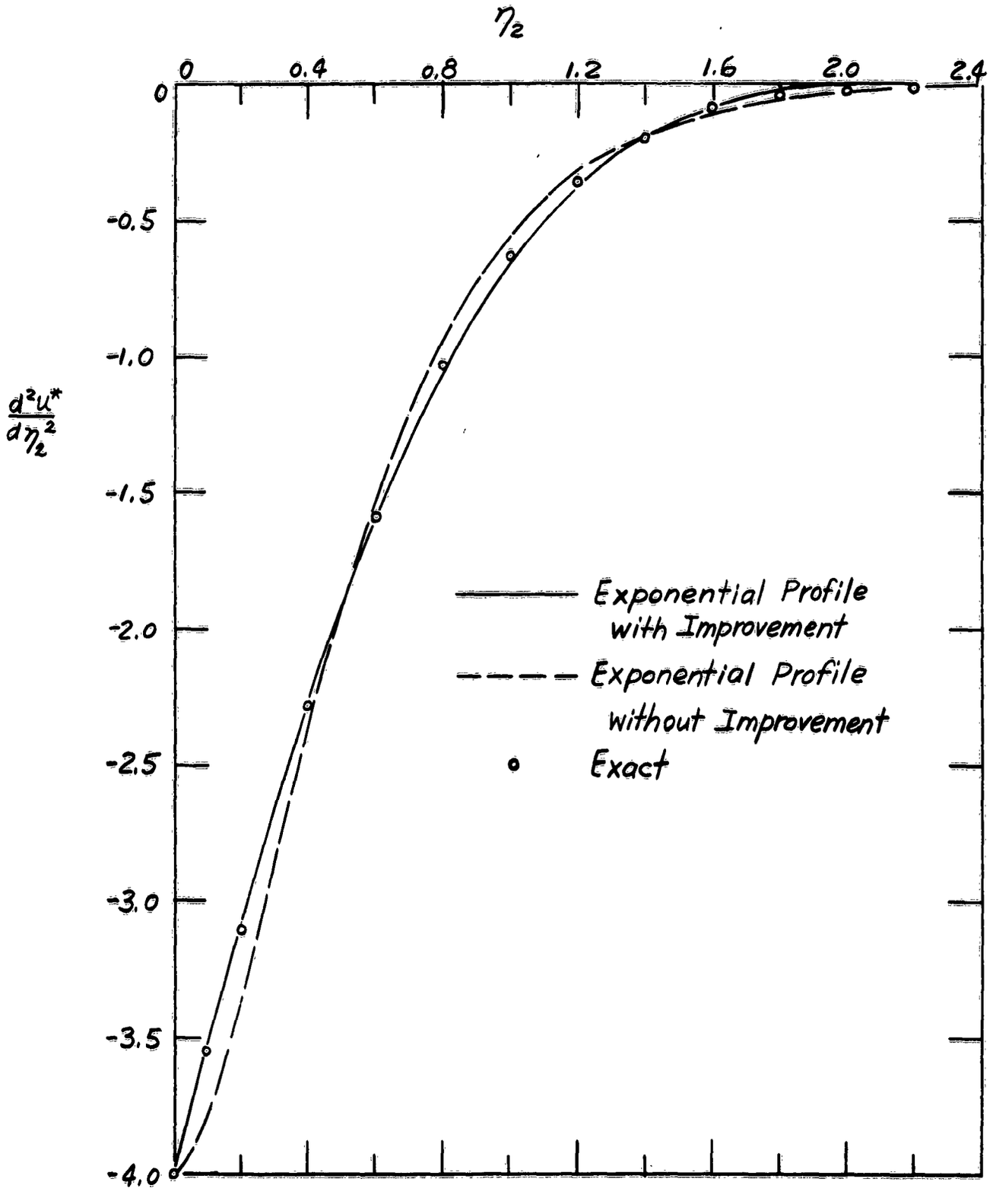
η_2
0
0.4
0.8
1.2
1.6
2.0
2.4
0
-0.5
-1.0
-1.5
-2.0
-2.5
-3.0
-3.5
-4.0
$\frac{d^2u^*}{d\eta_2^2}$
Exponential Profile with Improvement
Exponential Profile without Improvement
Exact

FIG. 8.

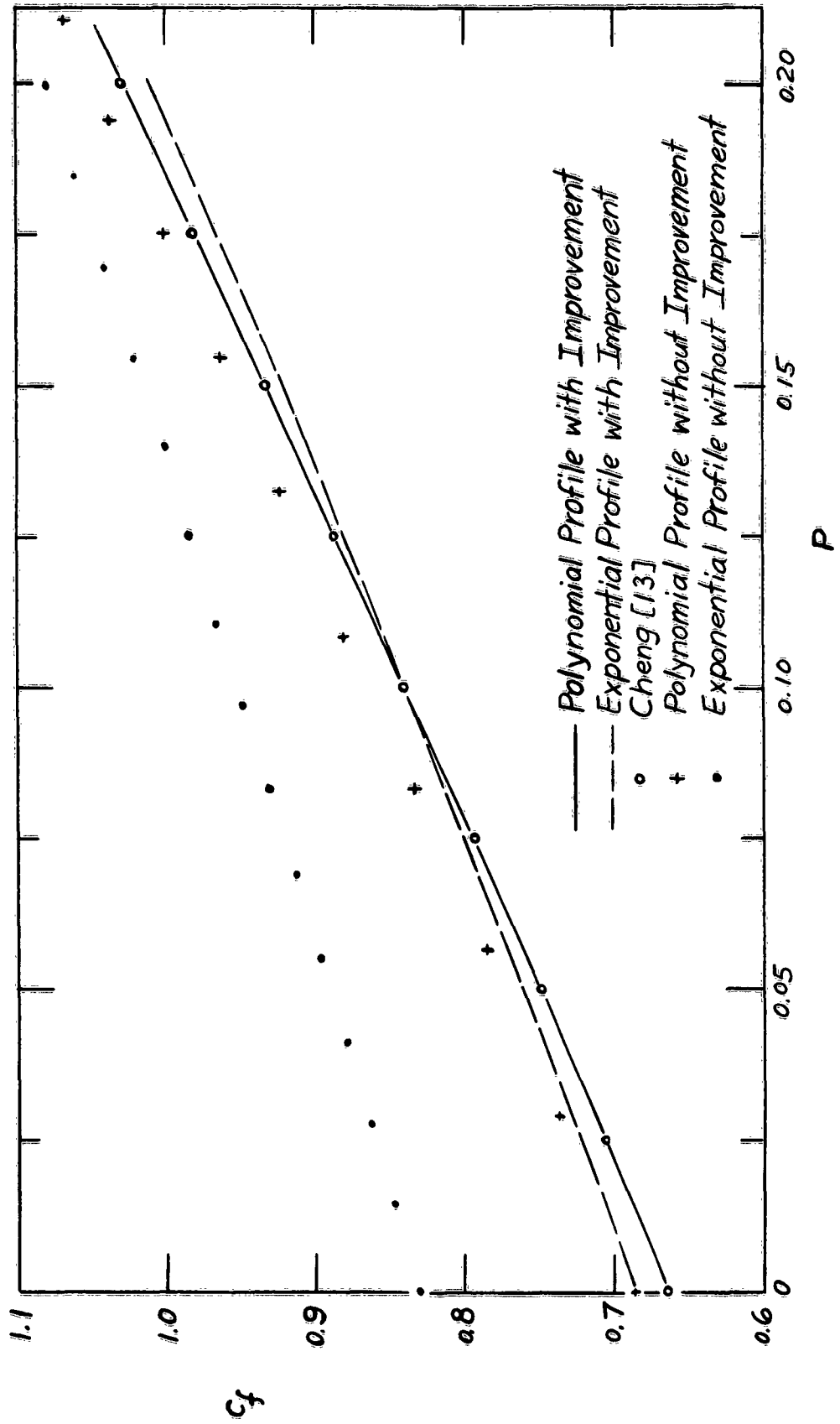
Polynomial Profile with Improvement
Exponential Profile with Improvement
Cheng [13]
Polynomial Profile without Improvement
Exponential Profile without Improvement
C_f
P
1.1
1.0
0.9
0.8
0.7
0.6
0
0.05
0.10
0.15
0.20

FIG. 9.

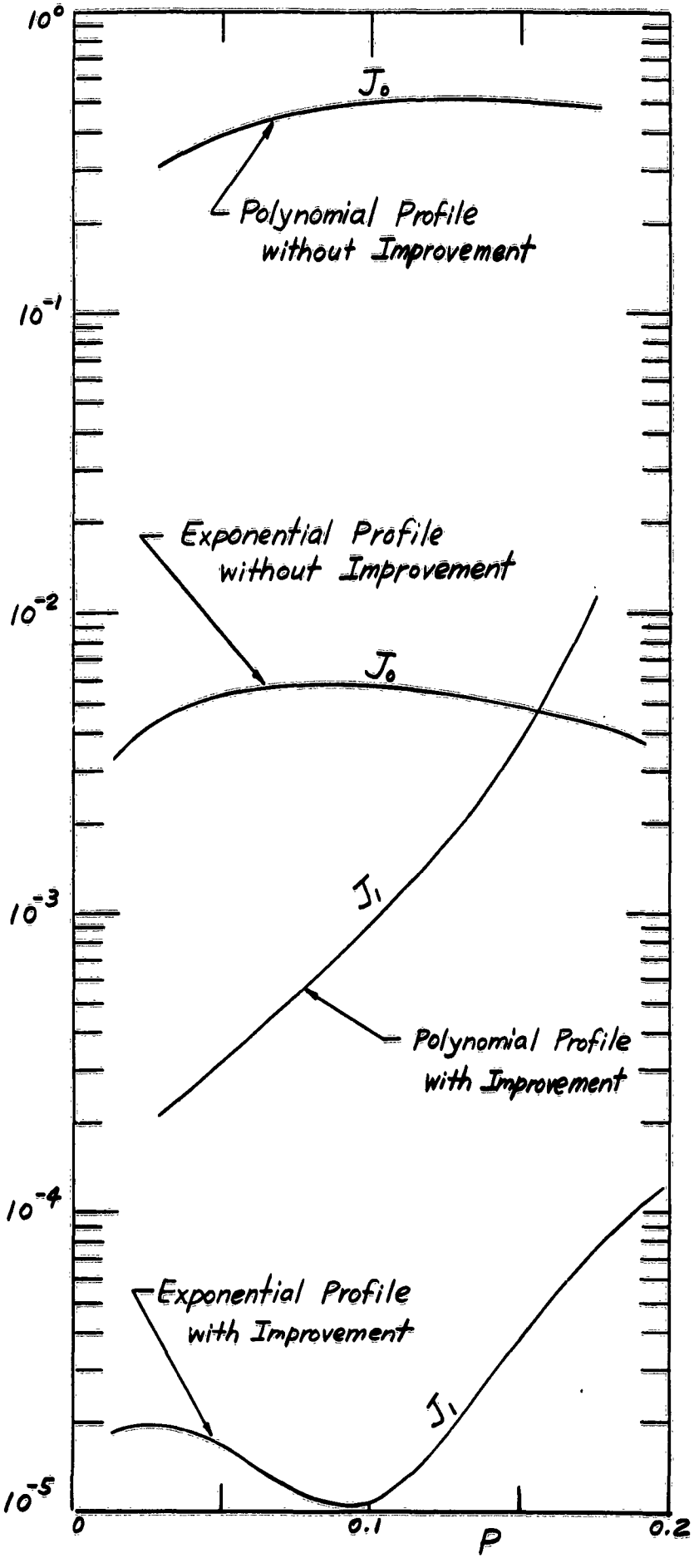
10^0
10^{-1}
10^{-2}
10^{-3}
10^{-4}
10^{-5}
J_0
Polynomial Profile
without Improvement
Exponential Profile
without Improvement
J_0
J_1
Polynomial Profile
with Improvement
Exponential Profile
with Improvement
J_1
0
0.1
0.2
P

FIG. 10.

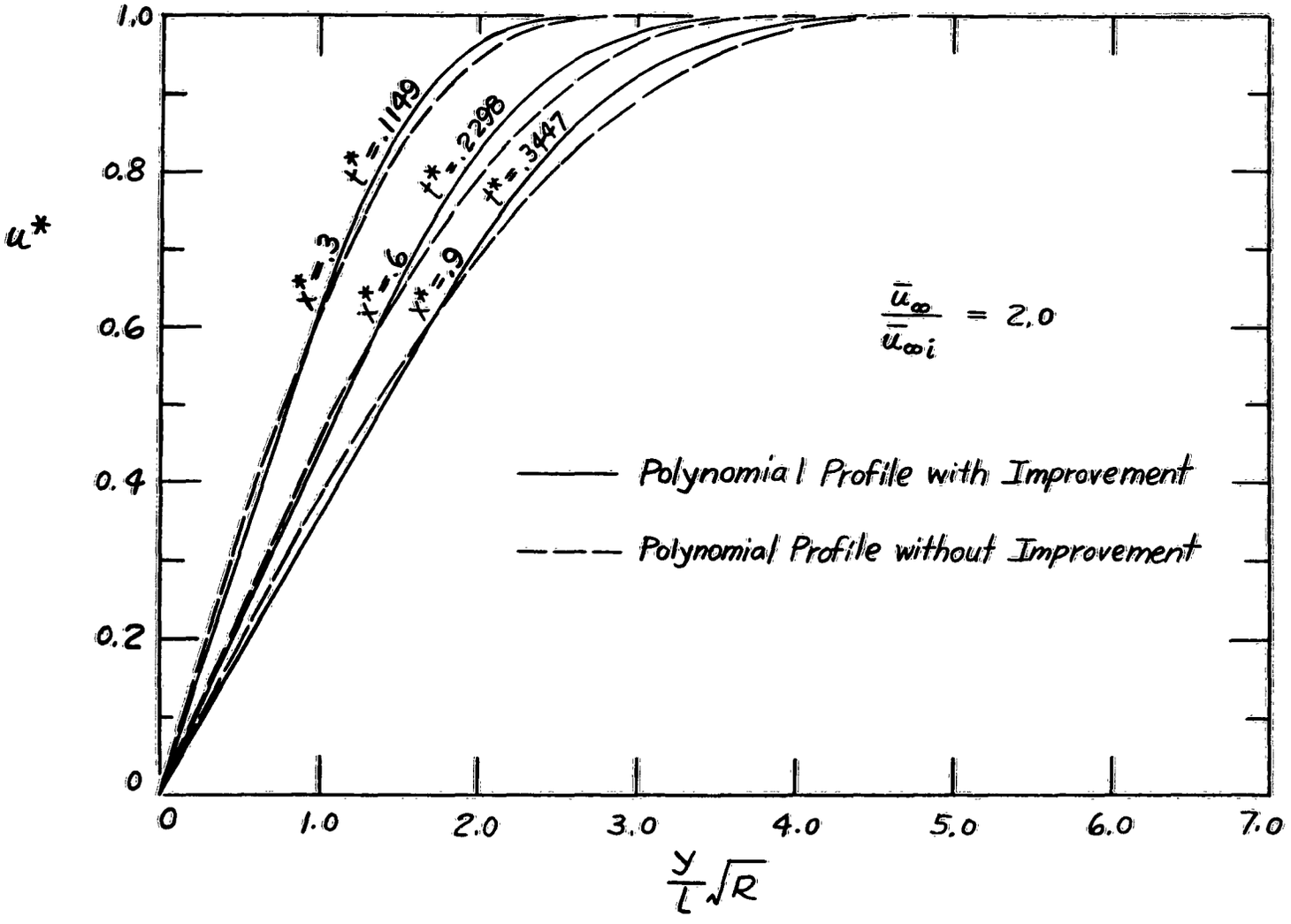
1.0
0.8
0.6
0.4
0.2
0
u*
0
1.0
2.0
3.0
4.0
5.0
6.0
7.0
$\frac{y}{l}\sqrt{R}$
x*=.3
x*=.6
x*=.9
t*=.1149
t*=.2298
t*=.3447
$\frac{\bar{u}_\infty}{\bar{u}_{\infty i}} = 2.0$
Polynomial Profile with Improvement
Polynomial Profile without Improvement

FIG. 11.

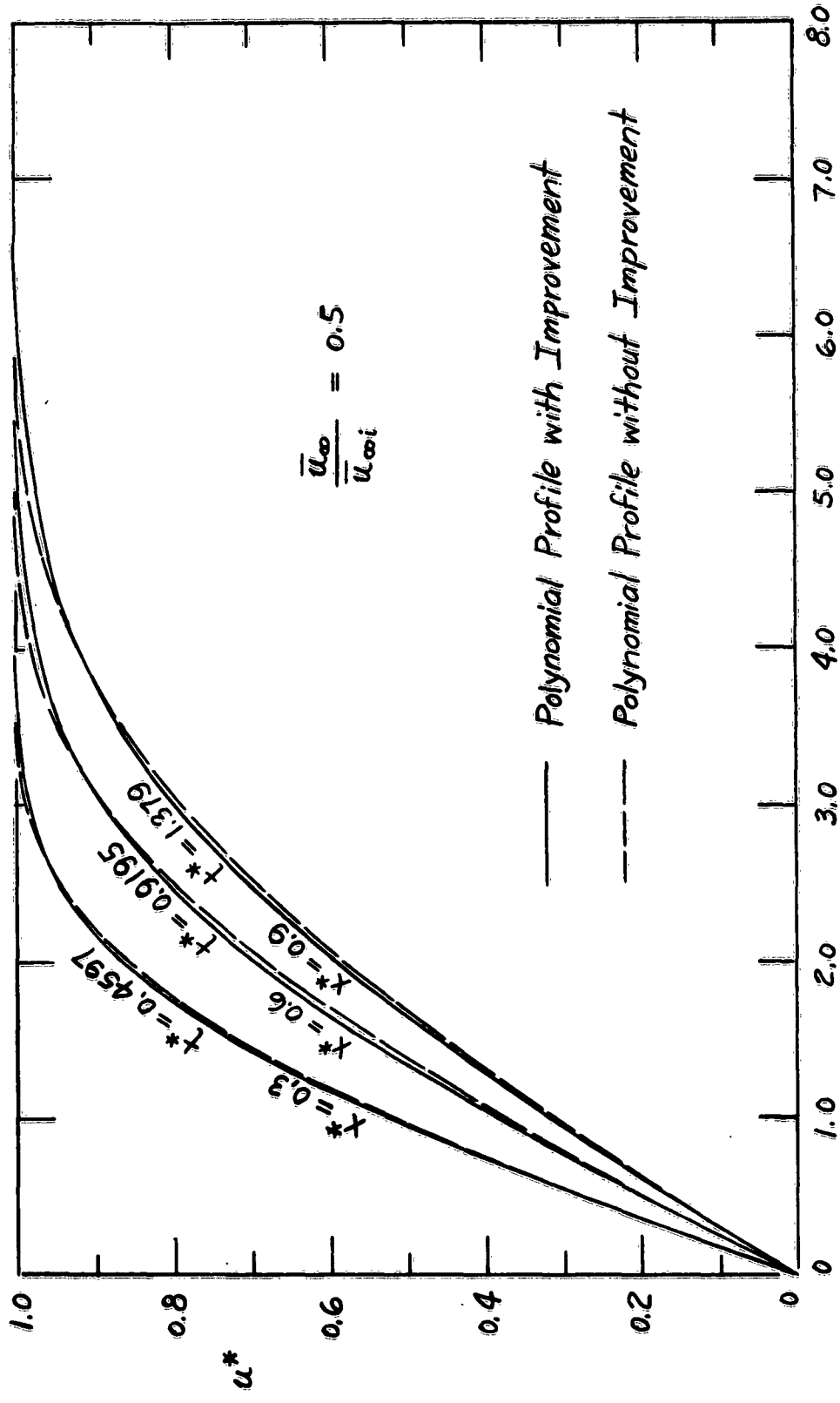
$\frac{\bar{u}_\infty}{\bar{u}_{\infty i}} = 0.5$
Polynomial Profile with Improvement
Polynomial Profile without Improvement
$x^* = 0.3$
$x^* = 0.6$
$x^* = 0.9$
$t^* = 0.457$
$t^* = 0.9195$
$t^* = 1.379$
u^*
$\frac{y}{L}\sqrt{R}$
0
0.2
0.4
0.6
0.8
1.0
1.0
2.0
3.0
4.0
5.0
6.0
7.0
8.0

FIG. 12.

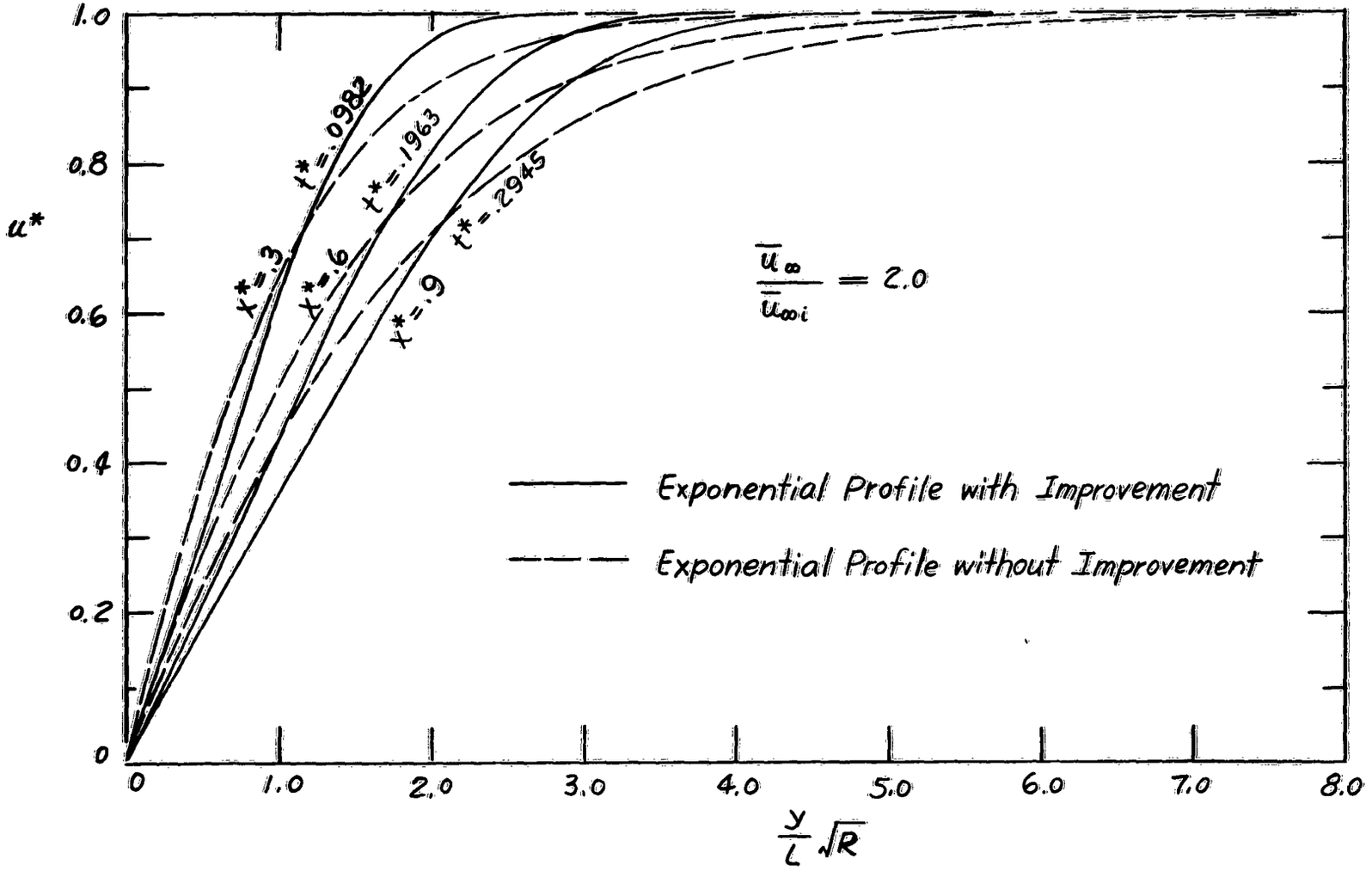
1.0
0.8
0.6
0.4
0.2
0
u*
0
1.0
2.0
3.0
4.0
5.0
6.0
7.0
8.0
$\frac{y}{L}\sqrt{R}$
x*=.3
t*=.0982
x*=.6
t*=.1963
x*=.9
t*=.2945
$\frac{\bar{u}_\infty}{\bar{u}_{\infty i}} = 2.0$
Exponential Profile with Improvement
Exponential Profile without Improvement

FIG. 13.

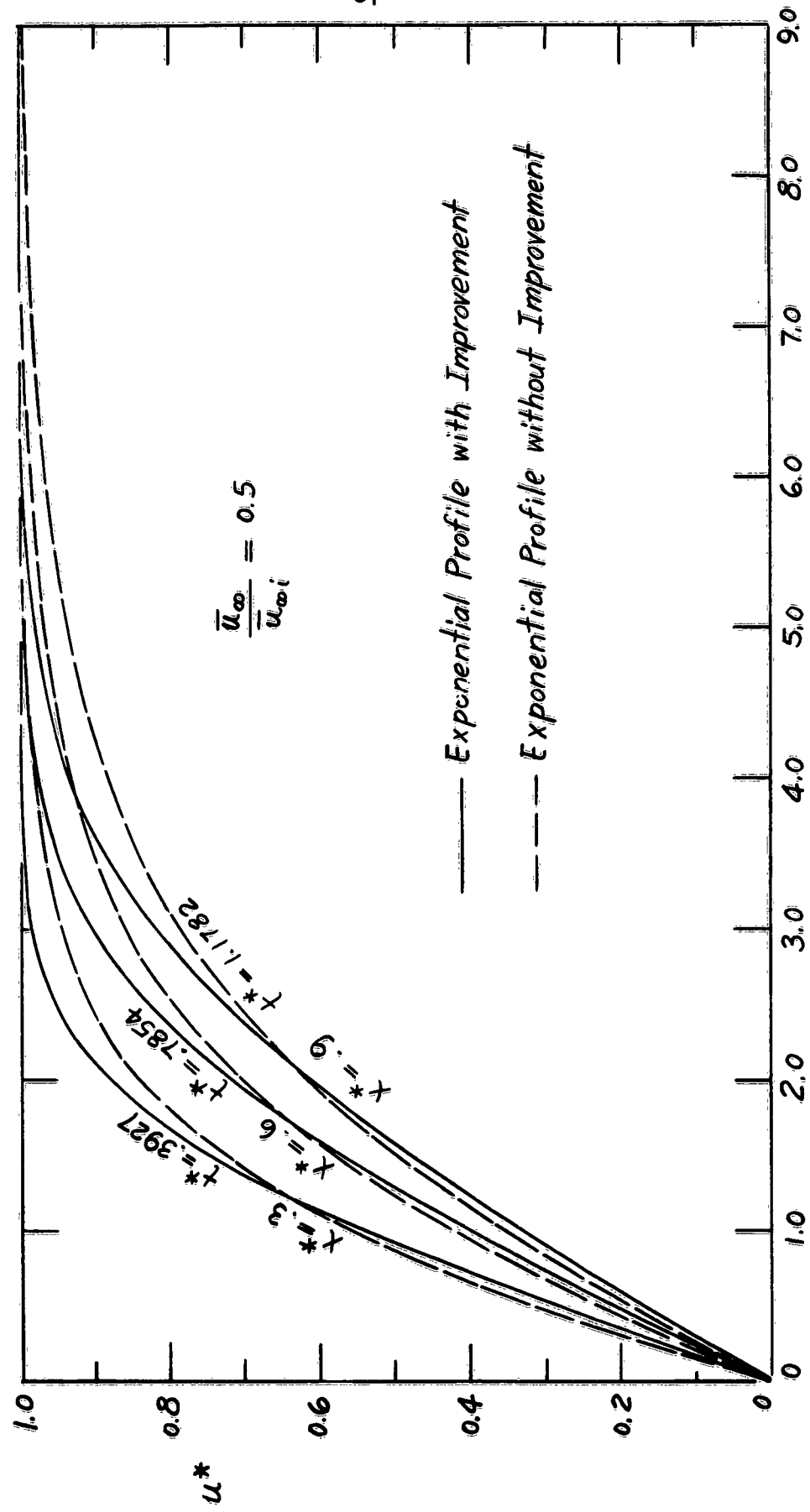
Exponential Profile with Improvement
Exponential Profile without Improvement
$\frac{\bar{u}_\infty}{\bar{u}_{\infty i}} = 0.5$
$x^* = .3$
$x^* = .6$
$x^* = .9$
$x^* = 1.1782$
$t^* = .3927$
$t^* = .7854$
$t^* = 1.1782$
u^*
$\frac{y}{L}\sqrt{R}$
0
0.2
0.4
0.6
0.8
1.0
1.0
2.0
3.0
4.0
5.0
6.0
7.0
8.0
9.0

FIG. 14.

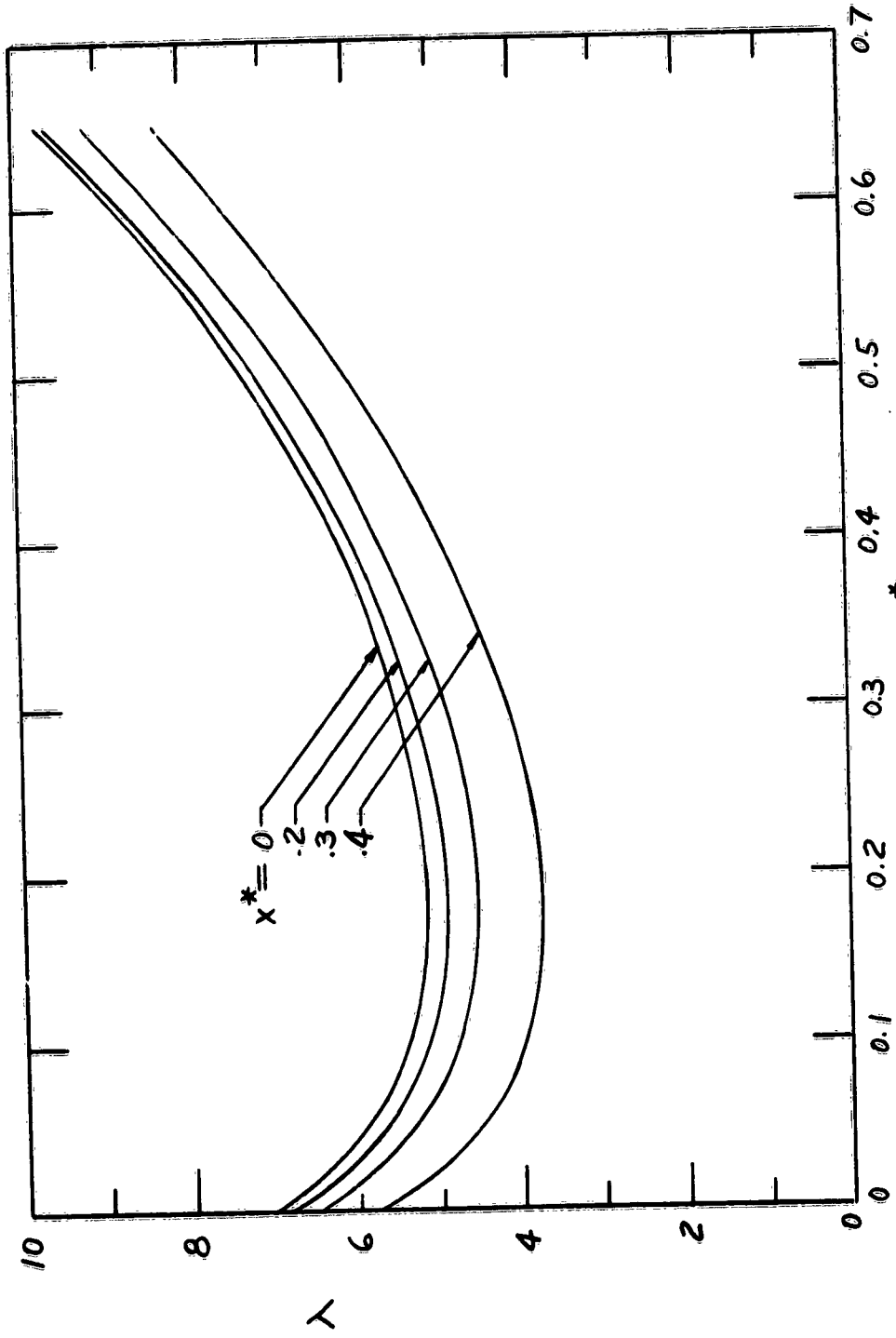

FIG. 15.

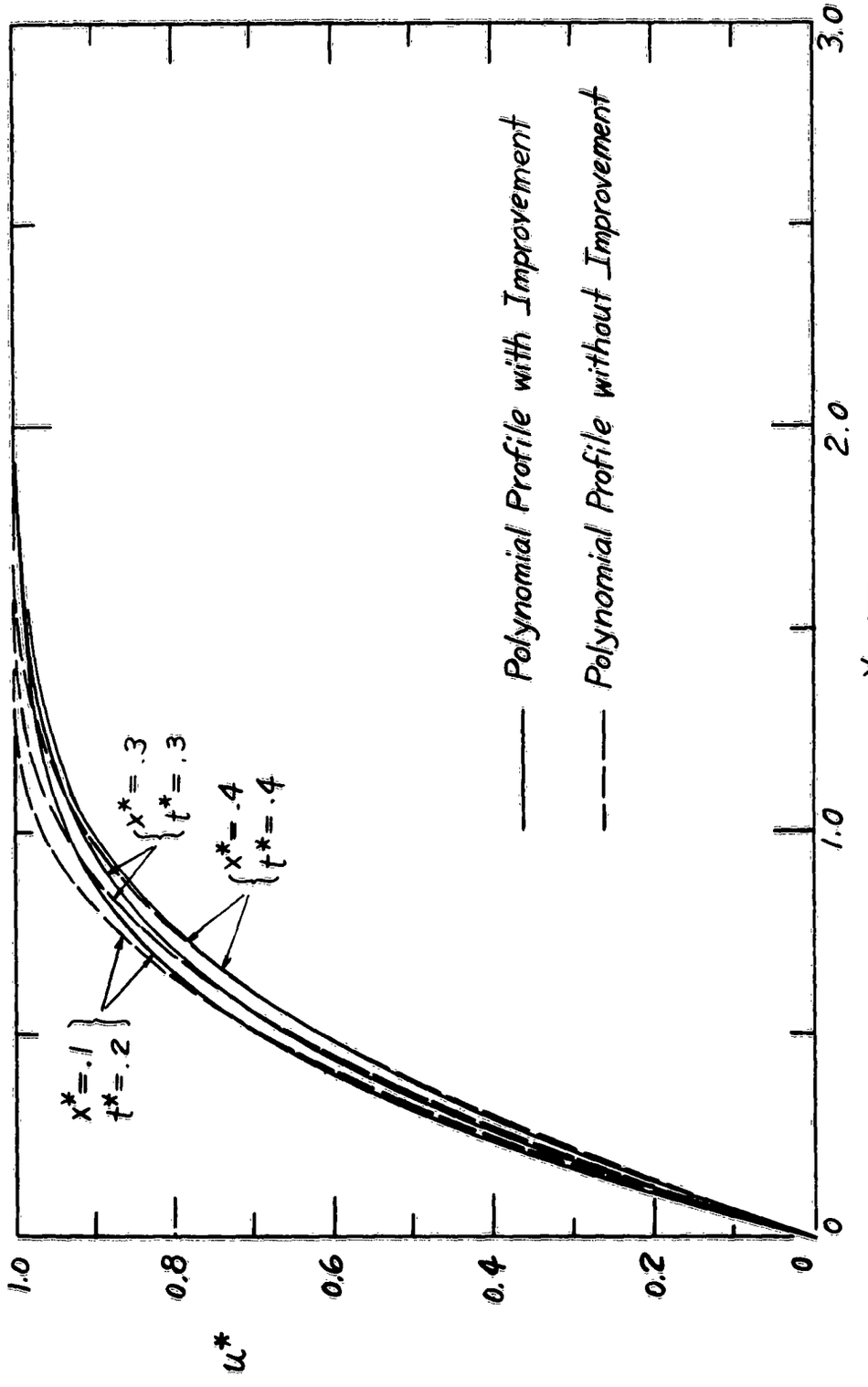
Polynomial Profile with Improvement
Polynomial Profile without Improvement
x*=.1
t*=.2
x*=.3
t*=.3
x*=.4
t*=.4
u*
y/L √R
0
0.2
0.4
0.6
0.8
1.0
1.0
2.0
3.0

FIG. 16.

DISTRIBUTION LIST

No. of Copies	
75	Director, DTMB Washington 7, D.C. Attention: Code 513
1 1	Office of Naval Research Washington 25, D.C. Attn: Head, Mechanics Br. Attn: Head, Fluid Dynamics Br.
1	Commander, U. S. NOTS China Lake, Calif. Attn: Technical Library
1	Office of Naval Research Branch Office 80 E. Randolph Street Chicago 1, Illinois Attn: Mr. M. A. Chaszeyka
1	Office of Naval Research Field Representative Room 233, Executive Bldg. Purdue University Lafayette, Indiana Attn: Mr. E. F. Schneider
1	Office of the Assistant Secretary of Defense (R&D) The Pentagon Washington 25, D.C. Attn: Technical Library
1	ASTIA Arlington Hall Station Arlington 12, Virginia Attn: TIPDR
1	Commanding General Aberdeen Proving Ground, Md. Attn: Technical Info. Brandh
1	Commander, WADC Wright-Patterson AF Base Ohio Attn: Library

No. of Copies	
1	NASA High Speed Flight Sta. Box 273 Edwards AF Base, Calif. Attn: Mr. W. C. Williams
1	NASA Ames Research Center Moffet Field, Calif. Attn: Librarian
1	NASA Langley Aero. Laboratory Langley Field, Virginia Attn: Librarian
1	NASA Lewis Flight Propulsion Lab. 21000 Brookpark Road Cleveland 11, Ohio Attn: Librarian
1	NASA 1520 H Street, N.W. Washington 25, D.C. Attn: Chief, Division of Research Information
1	Office, Chief of Ordnance Department of the Army Washington 25, D.C. Attn: Technical Library
1	Director U.S. Naval Ordnance Lab. White Oak, Maryland Attn: Technical Library
1 1	Case Institute of Tech. Cleveland 6, Ohio Attn: Prof. G. Kuerti Attn: Prof. S. Ostrach
1 1	Massachusetts Institute of Technology Cambridge 39, Mass. Attn: Dr. C. C. Lin Attn: Dr. A. Shapiro

No. of Copies	
	Commanding General Arnold Engineering Development Center Tullahoma, Tennessee
1	Attn: Technical Library
	Commanding General Army Ballistic Missile Agency Huntsville, Alabama
1	Attn: Technical Library
	University of Minnesota Dept. of Mechanical Engineering Minneapolis 14, Minnesota
1	Attn: Heat Transfer Laboratory
1	Attn: St. Anthony Falls Hydraulic Laboratory
	Institute for Fluid Dynamics and Applied Mathematics University of Maryland College Park, Maryland
1	Attn: Dr. F. Hama
	University of Michigan Ann Arbor, Michigan
1	Attn: Dr. C. S. Yih
1	Attn: Dr. J. A. Clark
1	Attn: Dr. A. Hanson
	Cornell University Ithaca, New York
1	Attn: Dr. S. F. Shen
1	Attn: Dr. B. Gebhart
	The Johns Hopkins University Charles and 34th Streets Baltimore, Maryland
1	Attn: Dr. M. V. Morkovin
	George C. Marshall Space Flight Center Huntsville, Alabama
1	Attn: Dr. E. W. Adams
	Cornell Aeronautical Lab., Inc. 4455 Genesee Street Buffalo 21, New York
1	Attn: Dr. Franklin Moore

No. of Copies	
	Polytechnic Institute of Brooklyn 527 Atlantic Avenue Freeport, New York
1	Attn: Dr. P Libby
1	Attn: Dr. M. Bloom
	Brown University Division of Engineering Providence, Rhode Island
1	Attn: Dr. J. Kestin
	National Bureau of Standards Washington 25, D.C.
1	Attn: Chief, Fluid Mechanics Section
	North American Aviation, Inc. Aerophysics Laboratory Downing, California
1	Attn: Dr. E. R. Van Driest
	Boeing Airplane Co. Seattle, Washington
1	Attn: Dr. J. C. Y. Koh
	University of Tennessee Ext. Arnold AF Base Tullahoma, Tennessee
1	Attn: Dr. M. K. Newman
	General Electric Co. Missile and Space Vehicle Dept. 3198 Chestnut Street Philadelphia, Pa.
1	Attn: Dr. S. M. Scala
1	Attn: Dr. H. Lew
	Armour Research Foundation 10 W. 35th Street Chicago 16, Illinois
1	Attn: Dept. M.
	Georgia Institute of Technology Atlanta, Georgia
1	Attn: Dean M. J. Goglia

No. of Copies

California Institute of Technology
Pasadena, California
1 Attn: GALCIT, Aeronautics Library
1 Attn: Jet Propulsion Lab.

Applied Mechanics Reviews
Southwest Research Institute
8500 Culebra Road
San Antonio, Texas
1 Attn: Dr. S. Juharz

Oceanics, Inc.
Technical Industrial Park
1 Plainview, L.I., New York

Mechanical Technology, Inc.
968 Albany-Shaker Rd.
Latham, New York
1 Attn: Dr. C. H. T. Pan

University of Notre Dame
Dept. of Mechanical Engineering
Notre Dame, Indiana
15 Attn: Department Secretary
1 Attn: Dr. E. W. Jerger
1 Attn: Dr. A. A. Szewczyk

Princeton University
Dept. of Aeronautical Eng.
Princeton, New Jersey
1 Attn: Dr. S. I. Cheng
School of Engineering
1 Prof. C. S. Mellor

Stanford University
Dept. of Mechanical Engineering
Stanford, California
1 Attn: Dr. S. Kline

Tulane University
Dept. of Mechanical Engineering
New Orleans, Louisiana
1 Attn: Dr. H. Sogin

Purdue University
Dept. of Mechanical Engineering
Lafayette, Indiana
1 Attn: Dr. R. J. Grosh

No. of Copies

State University of New York at Stony Brook
College of Engineering
Stony Brook, New York
1 Attn: Dr. T. F. Irvine, Jr.

Commanding Officer
Office of Naval Research
Branch Office
495 Summer Street
1 Boston, Massachusetts

Commanding Officer
Office of Naval Research
Branch Office
207 W. 24th Street
1 New York 11, New York

Commanding Officer
Office of Naval Research
Branch Office
1000 Geary Street
1 San Francisco 9, California

Chief, Bureau of Ships
Department of the Navy
Washington 25, D.C.
1 Attn: Code 341B
1 " 345
3 " 421
1 " 430
1 " 320

Librarian
Society of Naval Architects and Marine Engineers
74 Trinity Place
1 New York 6, New York

Douglas Aircraft Company
Aircraft Division
Longbeach, California
1 Attn: Mr. A. M. O. Smith

Dept. of Mechanical Engineering
Aeronautical Laboratory
Illinois Institute of Technology
Technology Center
Chicago 16, Illinois
1 Attn: Dr. A. A. Fejer, Director

No. of
Copies

Bolt Beranek and Newman, Inc.
50 Moulton Street
Cambridge 38, Massachusetts
1 Attn: Dr. F. J. Jackson

Department of Civil Engineering
Colorado State University
Research Foundation
Fort Collins, Colorado
1 Attn: Mr. E. J. Plate

Department of Theoretical and
Applied Mechanics
University of Illinois
Urbana, Illinois
1 Attn: Professor J. M. Robertson

Commanding Officer
Office of Naval Research
Branch Office
1030 East Green Street
1 Pasadena, 1, California